THE ASTROPHYSICAL JOURNAL SUPPLEMENT SERIES, 82:167–195, 1992 September

MODELS OF GAS-GRAIN CHEMISTRY IN DENSE INTERSTELLAR CLOUDS WITH COMPLEX ORGANIC MOLECULES

TATSUHIKO I. HASEGAWA AND ERIC HERBST
Department of Physics, The Ohio State University, 174 West 18th Avenue, Columbus, OH 43210
AND
CHUN MING LEUNG
Department of Physics, Rensselaer Polytechnic Institute, Troy, NY 12180-3590
Received 1991 November 20; accepted 1992 February 11

ABSTRACT

Models of the chemistry of dense interstellar clouds are presented in which both gas-phase and grain-surface chemistry occur. The dust grain and gas temperatures are fixed at 10 K, and the gas density $n = n(\mathrm{H}) + 2n(\mathrm{H_2})$ remains approximately at 2×10^4 cm^{-3} in these models, which are designed primarily to represent the chemistry occurring in dark clouds. We utilize previous ideas on what constitutes the most likely reactions to occur on large classical grains. Grain reactions that produce molecules as complex as those in our previous models of gas-phase chemistry are included to help elucidate the role of grains in the synthesis of organic molecules. The only desorption process allowed is thermal evaporation, so that heavy neutral species remain on the grain surfaces. The time-dependent gas-grain chemistry is followed by solving coupled differential equations. Three different sets of initial gas-phase abundances are assumed: steady state abundances, as calculated in our earlier gas-phase models; neutral atomic abundances; and the standard initial abundances utilized in pseudo–time-dependent gas-phase calculations, in which hydrogen is mainly molecular. Results as a function of time are presented for the different initial cloud compositions and compared both with previous, more restricted calculations of this type and with available observations. Among our conclusions is that a homogeneous gas-grain model for dark interstellar clouds can represent adequately observed abundances on grain surfaces (e.g., H_2O, CH_4) as well as in the gas at so-called early time. We also conclude that significant abundances of complex organic molecules can be synthesized on grain surfaces from gaseous precursors of varying complexity.

Subject headings: dust, extinction — ISM: clouds — ISM: molecules — molecular processes

1. INTRODUCTION

There is a growing body of observational evidence, based on broad but strong infrared features, that significant amounts of volatile molecules such as CO, H_2O, and CH_4 reside on the surfaces of dust grains in dense interstellar clouds (Lacy et al. 1984; Whittet & Duley 1991; Knacke & Larson 1991; Lacy et al. 1991; Tielens et al. 1991) as well as in the gas phase. The surface molecules can be formed either in the gas phase via ion-molecule reactions followed by accretion onto the dust particles, or via direct production on the grain surfaces. There is also increasing observational evidence that selected gas-phase molecules in the interstellar medium more complex than H_2 are produced at least in part on the surfaces of dust particles and then desorbed into the gas. The recent observation of NH in diffuse clouds (Meyer & Roth 1991) and the ubiquity of H_2CO in exterior portions of dense clouds (Federman & Allen 1991) can both be plausibly explained by grain-surface chemistry, although the desorption mechanisms are not well understood. In dense/compact regions such as the well-studied hot core source in Orion, high abundances of selected saturated molecules such as NH_3, H_2O, and more complex species in the gas phase (Walmsley et al. 1987; Blake et al. 1987) indicate another formation mechanism in addition to ion-molecule chemistry. Surface hydrogenation via H atoms followed by thermal evaporation due to rising temperatures is a reasonable possibility (Pauls et al. 1983; Brown, Charnley, & Millar 1988). The high degree of deuteration found in the hot core has also been explained in terms of surface chemistry (Brown & Millar 1989a,b; Turner 1990).

The study of surface reactions in the interstellar medium has a long history. Salpeter and colleagues studied the formation of H_2 on grain surfaces in some detail (e.g., Hollenbach & Salpeter 1970). This work was followed by that of Watson & Salpeter (1972a,b), who considered mainly hydrogenation reactions between mobile H atoms and more stationary heavy atoms and radicals to form saturated species such as CH_4, NH_3, and H_2O. Similar research was undertaken by Aannestad (1973). Watson (1976) later provided a useful review of grain chemistry and desorption mechanisms. Allen & Robinson (1975, 1976; 1977, hereafter AR) considered a wide assortment of surface association reactions without activation energy, typically occurring between radicals, to produce some rather complex species. Although the surface migration of most of these reactants is not rapid, the grains considered by AR are small, so that reaction rates are still appreciable. Desorption from the small grains occurs via transient heating of the whole grain resulting from the exothermicity of chemical reactions, followed by evaporation. Although AR used pure grain-surface chemistry to explain gas-phase molecular abundances, in their model the gaseous molecules are not destroyed by gas-phase reactions but only depleted via grain adsorption.

Tielens & Hagen (1982, hereafter TH) studied the chemical

evolution of grain mantles using steady state gas-phase abundances and a model for grain chemistry on large ("classical") grains in which the relative rates of surface migration are important so that simple atoms such as H, C, N, and O, which tend to migrate more rapidly than heavy molecular species, dominate the chemistry. Molecular hydrogen formation occurs through a variety of hydrogen abstraction reactions in addition to H + H association. Desorption of heavy species does not occur; rather, grain mantles build up. Later, Tielens & Allamandola (1987, hereafter TA) wrote a lengthy and useful review on their views of interstellar surface chemistry. D'Hendecourt, Allamandola, & Greenberg (1985) modeled the gas and grain chemistry simultaneously for a limited number of species. In their model, a steady state between the grain-surface and gaseous molecular abundances is maintained by desorption of surface molecules via grain explosions and photodesorption. The role of grain processes in a complex gas-grain model of the chemistry in T Tauri wind-blown bubbles has been studied by Charnley et al. (1988).

More recently, Brown (1990) has given another view of how complex molecules might be formed on grain surfaces; in this picture the exothermicity of chemical reactions can be channeled into translational energy of reaction products, so that even heavy radicals can migrate appreciably and react subsequently. For example, the methyl (CH_3) and hydroxyl (OH) radicals, produced via exothermic reactions, can migrate sufficiently to associate and form methanol (CH_3OH). If the ideas of Brown (1990) are followed, the radical reactions considered by AR can occur on large grains. The AR and Brown (1990) views of surface chemistry are thus much less restrictive in the variety of rapid reactions allowed than the views of TH and TA. Clearly, there is still much uncertainty regarding the dominant grain reactions and their rates.

Despite the work outlined above, in recent years the study of grain reactions has been comparatively neglected because of the success of exceedingly detailed gas-phase models in reproducing observed chemical abundances in dense interstellar clouds. While the need to include grain chemistry has been felt by many practitioners, it has played a significant role mainly in models of the chemistry of star formation regions (e.g., Brown et al. 1988). The trend for ambient (quiescent) regions has been to pursue the gas-phase approach to determine what it can and cannot explain. Recent reviews on the successes and failures of gas-phase models have been given by Herbst (1990) and Herbst & Millar (1991). In addition to so-called pseudo–time-dependent gas-phase models, in which chemical abundances evolve under fixed physical conditions, gas-phase models with complex dynamical processes representing inhomogeneous regions (Millar, Herbst, & Charnley 1991; Chièze, Pineau des Forêts, & Herbst 1991) and hydrodynamics (Prasad, Heere, & Tarafdar 1991) also exist. In recent years, the depletion of gas-phase molecules onto grain surfaces has been included in a few gas-phase models. In the absence of rapid nonthermal desorption processes, the amount of time available for gas-phase chemistry is reduced and the chemistry altered somewhat (Brown & Charnley 1990; Pineau des Forêts, Flower, & Herbst 1991). Although these studies rule out the use of steady state ($t \geq 1 \times 10^7$ yr) strictly gas-phase treatments, since steady state abundances take too long to achieve, they also show that so-called early-time ($t \approx 10^5$–10^6 yr) gas-phase results are not affected as greatly. Brown & Charnley (1991) have shown, for example, how the formation of methane (CH_4) on grain surfaces followed by desorption affects the early time-dependent gas-phase chemistry only to a limited degree.

Given the recent depth of work on gas-phase chemistry, we feel that it is appropriate now to present a more thorough treatment of the role of grain chemistry and its interaction with gas-phase chemistry in ambient dense interstellar clouds than has been attempted heretofore. We are especially interested in the role grain surfaces might play in producing "complex" molecules such as the cyanopolyynes. Because there remains great uncertainty on what processes occur and how rapidly they occur on grain surfaces, we do not expect the results presented here to have the same reliability as those that are derived from a purely gas-phase calculation. However, they represent our first serious attempt to incorporate the chemical ramifications of grains in interstellar clouds. Starting with the large gas-phase reaction network of Herbst & Leung (1989, 1990; hereafter HL1, HL2, respectively), we have added a significant number of grain-surface reactions involving molecules as complex as 10 heavy atoms and solved the pseudo–time-dependent chemistry for a physical environment appropriate to a dark cloud such as TMC-1. In general, we have adopted the rather restrictive viewpoint of TH and TA in constructing our grain-surface reaction network. Nonthermal desorption mechanisms are not considered in this initial treatment. A variety of different initial abundances are assumed, and different and highly complex grain chemistries result.

The remainder of the paper is divided as follows. In § 2 we discuss the details of the grain processes and reactions in our model, while in § 3 the results and chemical pathways are considered. In § 4 the results are compared with observations and those obtained from previous, more restricted calculations. A summary is contained in § 5.

2. MODEL

In the present work, we have added a series of grain-surface reactions to the extensive pseudo–time-dependent gas-phase chemical models of HL1 and HL2. These surface reactions involve molecules as complex as those in the gas-phase network. The elemental abundances chosen for the gaseous and surface species are the so-called depleted metal abundances (Leung, Herbst, & Huebner 1984). In the gas-phase reactions, rapid ion-polar rates are utilized when appropriate (Herbst & Leung 1986).

We consider only atoms and molecules that are physisorbed (weakly adsorbed) onto so-called classical dust grains, which are characterized by a radius of 1000 Å, a density of 3 g cm^{-3}, and 10^6 surface sites for adsorption. With a gas-to-dust ratio of 100 by mass, the number density of the grains, n_d, is $1.33 \times 10^{-12} n$, where n is the concentration of H nuclei in all forms. It is generally believed that in dense cold clouds such as TMC-1, the gas kinetic temperature T_k and the dust temperature T_d are both about 10 K, a value used here. We assume a sticking probability of 1.0 for all neutral atoms and molecules that strike a grain. The accretion rate for a given neutral species i, $R_{acc}(i)$, in units of cm^{-3} s^{-1}, is then given by

$$R_{\rm acc}(i) = \sigma_d \langle v(i) \rangle n(i) n_d \,, \quad (1)$$

where $n(i)$ is the concentration of species i, $\langle v(i) \rangle$ is its thermal velocity, and σ_d is the geometrical dust-grain cross section. It is not certain whether molecular and atomic ions stick to the grain surfaces (Watson 1976). We assume that they do not. In the gas-phase chemical models of HL1 and HL2, which are incorporated with minor modifications into this work, sticking of electrons to neutral grains is included as well as ion-electron recombinations on negatively charged grains, leading to gaseous products. In our present model, the charge on the grain (0 or −1) does not influence the chemistry, which solely involves neutral species.

The neutral species are bound to the grain surface with a binding energy for physical adsorption, E_D, of order 1000 K or 0.1 eV (TH; TA). The actual adsorption energies adopted here for atoms and simple molecules are given in Table 1. These are taken from previous sources and represent estimates for binding energies on a graphite surface (AR) or an icy surface with some H_2 (TA). A much larger table of adsorption energies for more complex species is given by AR; however, the values excluded from Table 1 are not needed in our calculations, as discussed below. Clearly, the E_D values are dependent on the material making up the grains, in which case they should change somewhat as the grains evolve during the long lifetimes of interstellar clouds. Such higher order effects are neglected here.

On the grains, exothermic surface reactions occur, as discussed by numerous authors (Watson 1976; AR; TH; TA; etc.). In order to react, the adsorbed species require mobility. The time scale $t_{\rm hop}$ for an adsorbed species to migrate from one surface site (a potential well) to an adjacent site via thermal hopping is given by the equation

$$t_{\rm hop} = \nu_0^{-1} \exp\left(E_b / kT_d\right) , \quad (2)$$

where ν_0 is the characteristic vibration frequency for the adsorbed species, which is assumed to be isotropic, and E_b is the potential energy barrier between adjacent surface potential energy wells (TH; TA; Watson 1976). We adopt the recent (TA) estimate that $E_b \approx 0.3 E_D$, although other estimates exist (Watson 1976). Although the characteristic frequency is often assumed to be the same for all species, we utilize the more accurate harmonic oscillator relation that

$$\nu_0 = (2 n_s E_D / \pi^2 m)^{1/2} \,, \quad (3)$$

where n_s is the surface density of sites ($\approx 1.5 \times 10^{15}$ cm^{-2}) and m is the mass of the adsorbed particle (TA). This equation gives values in the range 10^{12}–10^{13} s^{-1}.

The diffusion time $t_{\rm diff}$ required for an adsorbed particle to sweep over a number of sites equivalent to the whole grain surface is given by

$$t_{\rm diff} = N_s t_{\rm hop} \,, \quad (4)$$

where $N_s = 10^6$ is the total number of surface sites on a grain. If the diffusion rate $R_{\rm diff}$ is defined as the inverse of $t_{\rm diff}$, the surface reaction rate R_{ij} (cm^{-3} s^{-1}) between surface species i and j occurring due to classical diffusion can be expressed as

$$R_{ij} = \kappa_{ij} (R_{{\rm diff},i} + R_{{\rm diff},j}) N_i N_j n_d \,, \quad (5)$$

where N_i and N_j are the numbers of molecules of species i and j, respectively, on an average grain; κ_{ij} is the probability for the reaction to happen upon an encounter; and n_d is the dust-grain number density. The parameter κ_{ij} is unity for an exothermic reaction without activation energy (as undergone by atoms and/or radicals which make up the vast majority of the reaction set utilized). For an exothermic reaction with activation energy E_a and at least one light reactant (H, H_2), κ_{ij} can be approximated by the exponential portion of the quantum mechanical probability for tunneling through a rectangular barrier of thickness a (TH):

TABLE 1

ADSORPTION ENERGIES, EVAPORATION TIMES, AND DIFFUSION RATES

Species	E_D (K)	E_b (K)	$t_{\rm evap}$ (s)	$R_{\rm diff}$ (s^{-1})	References
H	350	100	5.3(+2)	5.1(+4) q	1
H_2	450	135	1.5(+7)	3.0(+3) q	1
He	100	30	2.8(−8)	4.0(+4)	2
C	800	240	4.3(+22)	4.9(−5)	1
N	800	240	4.6(+22)	4.5(−5)	1
O	800	240	4.9(+22)	4.2(−5)	1
S	1100	330	6.4(+35)	4.3(−9)	1
CH	645	196	2.2(+16)	3.5(−3)	3
NH	604	181	1.7(+14)	1.4(−2)	3
OH	1259	378	3.4(+42)	5.2(−11)	3
CH_2	956	287	2.5(+29)	4.5(−7)	3
NH_2	856	257	1.3(+25)	8.0(−6)	3
CH_3	1158	347	1.4(+38)	1.2(−9)	3
NH_3	1107	332	9.3(+35)	4.9(−9)	3

NOTES.—$a(\pm b)$ means to $a \times 10^{\pm b}$. E_D = Adsorption energy. E_b = Surface potential barrier between surface sites. $R_{\rm diff}$ = Surface diffusion rate. q = Quantum tunneling.

REFERENCES.—(1) Tielens & Allamandola 1987; (2) Tielens & Hagen 1982; (3) Allen & Robinson 1977.

$$\kappa_{ij} = \exp\left[-2(a/\hbar)(2\mu E_a)^{1/2}\right], \quad (6)$$

where μ is the reduced mass and a is taken as 1 Å. For actual calculations, the reaction rate R_{ij} can be expressed in terms of a rate coefficient k_{ij} ($cm^3\ s^{-1}$) analogous to those in gas-phase two-body reactions via the expression

$$R_{ij} = k_{ij} n_s(i) n_s(j), \quad (7)$$

where $n_s(i)$, the concentration of surface species i, is defined by the relation

$$n_s(i) = N_i n_d, \quad (8)$$

and the rate coefficient k_{ij} is given by

$$k_{ij} = \kappa_{ij}(R_{\mathrm{diff},i} + R_{\mathrm{diff},j})/n_d. \quad (9)$$

Given the large ($\gg kT_d$) potential barriers E_b for most complex species (including radicals), significant surface reaction rates are limited to reactions involving light atoms such as H, C, N, O or selected diatomic molecules that can migrate at meaningful rates. This is essentially the view of Tielens and collaborators (TH; TA). The possibility that the energy from exothermic reactions can be efficiently channeled into surface translational energy of reaction products, considered by Brown (1990), leads to a wider assortment of possible reactions. It is not considered here because we assume that this energy is efficiently coupled to the phonon structure of the grains.

For the light reactive species H and H_2, surface migration due to quantum tunneling is more rapid than that due to classical hopping. With the same approximation as in equation (6), the time scale t_q for quantum tunneling to an adjacent surface site separated by a barrier of thickness a is

$$t_q = \nu_0^{-1} \exp\left[(2a/\hbar)(2mE_b)^{1/2}\right]. \quad (10)$$

Although the diffusion time due to quantum tunneling is proportional to $N_s^{1/2}$ on a perfect lattice, the diffusion time on an irregular lattice can be expressed in the same manner as for classical diffusion (Watson 1976). Thus, the quantum diffusion time t'_{diff} and rate R'_{diff} are given by the equations $t'_{\mathrm{diff}} = N_s t_q$ and $R'_{\mathrm{diff}} = (t'_{\mathrm{diff}})^{-1}$. For $E_b = 100$ K and $a = 1$ Å, the diffusion time for an H atom over an entire grain due to quantum tunneling is 2×10^{-5} s, whereas the analogous time due to thermal hopping at 10 K is 7×10^{-3} s. The value of 2×10^{-5} s is obtained from equation (10); an alternative method using the Heisenberg uncertainty principle and the width of the state of the adsorbed molecule yields 1×10^{-6} s (Watson 1976). Quantum diffusion for heavier species (e.g., the atoms C, N, and O) is not considered here, in line with previous approaches, although it may represent a substantial contribution according to our simple estimates.

Adsorbed species come off the grain surfaces via a variety of desorption mechanisms. Thermal evaporation time scales t_{evap} can be estimated from the relation akin to equation (2) except for the replacement of E_b by E_D. These times are shown for the species in Table 1 for $T_d = 10$ K. Only H, H_2, and He have meaningful evaporation times; all other species remain on the grains for the low-temperature lifetime of clouds unless nonthermal desorption mechanisms prevail. In the present calculations, only thermal evaporation is considered. Our motivation for excluding nonthermal desorption mechanisms is several fold. In introducing grain chemistry into our previously pristine gas-phase chemical network, we wish to proceed in a seriatim fashion to see how the gas-phase abundances are affected by a consideration of grain chemistry. In addition, nonthermal desorption mechanisms and rates are still uncertain. Photodesorption rates are not well determined and are unlikely to be rapid in the interiors of dense, cold clouds, although they may play a role in cloud exteriors (Federman & Allen 1991). Transient temperature pulses and explosions induced by cosmic rays are efficient on carbonaceous or CO–dominated grain mantles, but not on water ice-dominated mantles (Léger, Jura, & Omont 1985). Direct ejection via the energy of exothermic chemical reactions is not well understood (e.g., Brown & Charnley 1991). Since the energy released in the exothermic reactions is assumed to be efficiently transferred to the grain body, and since the large grains considered here have a heat capacity large enough to prevent a dramatic rise in grain temperature due to this energy release, desorption via grain heating due to surface chemical reactions (AR) need not be considered.

2.1. *Surface Reaction Network*

The gas-phase and grain-surface chemistry considered here are coupled through the accretion and thermal evaporation processes. The rate equations for a species i in the gas phase with concentration $n(i)$ and on grain surfaces with concentration $n_s(i)$ are given by the expressions

$$dn(i)/dt = \sum_l \sum_j K_{lj} n(l) n(j) - n(i) \sum_j K_{ij} n(j) - R_{\mathrm{acc}}(i) + t_{\mathrm{evap}}(i)^{-1} n_s(i), \quad (11a)$$

$$dn_s(i)/dt = \sum_l \sum_j k_{lj} n_s(l) n_s(j) - n_s(i) \sum_j k_{ij} n_s(j) + R_{\mathrm{acc}}(i) - t_{\mathrm{evap}}(i)^{-1} n_s(i), \quad (11b)$$

where gas-phase rate coefficients are labeled with a capital K to distinguish them from surface rate coefficients. Equation (11a) is modified from the previous gas-phase models by the inclusion of accretion and evaporation terms. Equation (11b) is new; it represents the time-dependent chemistry of the surface species and includes formation, destruction, accretion, and evaporation terms. The gas-phase reaction network is the same as in HL2, except that the formation of H_2 is now handled explicitly via grain chemistry (i.e., via eq. [11b]). The numerical method utilized in solving the coupled differential equations from given initial abundances is the same as discussed by Leung et al. (1984). For some surface species there are no destruction terms via chemical reaction or desorption (evaporation occurs at a zero rate). This means that, unlike our gas-phase models, a true steady state can never be reached. The models, however, tend to reach asymptotic states in which important reactive heavy elements form dominant molecular products. The models are followed to a time of 1×10^7 yr only,

at which time most heavy elements and molecules are lost from the gas phase. Exceptions are metallic elements (d'Hendecourt et al. 1985), which are mainly charged and assumed not to stick to grain surfaces. For example, only one-fourth of the initial abundance of iron is on the grain surfaces at 1×10^7 yr, regardless of initial conditions.

There are 156 surface reactions in our network, involving 118 neutral species on the surface. These species are listed in Table 2 and include a greater variety of complex species, mainly more saturated (hydrogen-rich) ones, than our previous gas-phase models. The surface reactions and the adopted rate coefficients are listed in Table 3 along with references for those taken from earlier models. In addition to the surface species and reactions, there are 2575 gas-phase reactions in the model involving 274 gas-phase species. Note that the surface rate coefficients are much larger than their analogous gas-phase counterparts. Surface reactions occur rapidly in an absolute sense; it is the adsorption step which is the slow one. At the gas density considered, a species lands on a representative grain every ≈ 1–10 s and, if reactive, often reacts shortly thereafter. The reactions in our model involve at least one reaction partner (typically a first-row atom) which can migrate over the grain surface during an astrophysically meaningful time scale. First-row atomic species therefore have very low surface abundances. About half of the reactions are hydrogen addition (hydrogenation) reactions, leading to products typically more saturated than produced via gas-phase chemistry. Addition reactions involving atomic C and atomic N tend to convert simpler species into more complex hydrocarbons and cyanopolyynes. For example, reactions of the type $C + C_n \rightarrow C_{n+1}$ produce more complex carbon clusters, which can then be hydrogenated or react with N atoms to form cyanopolyynes. Reactions involving O atoms and carbon radicals to produce organo-oxygen species are typically not included, since the unsaturated oxygen-containing species that would be formed in addition reactions are mostly unknown. Another possibility is that reactions of the sort $C_n + O \rightarrow C_{n-1} + CO$ occur, as is assumed in our gas-phase models (HL1; HL2). Exclusion of these reactions makes carbon cluster growth on the grains more efficient than it would be if they were included. Indeed, exclusion of these reactions from the gas-phase network renders gas-phase chemistry far more efficient in organic synthesis (Millar, Leung, & Herbst 1987).

In our reaction set, the hydrogen addition reactions involving hydrocarbons ($H + C_nH_m \rightarrow C_nH_{m+1}$) possess no activation energy if the reactant hydrocarbon is a radical, i.e., contains an odd number of hydrogen atoms. Such species have an odd number of electrons, are almost always quite reactive, and have ground doublet electronic states. The hydrogen addition reactions possess some activation energy if the reactant hydrocarbon is "stable," i.e., contains a nonzero and even number of hydrogen atoms, and generally has a ground singlet state. Bare carbon clusters are quite reactive and are assumed to behave as radicals even if their ground electronic states possess singlet multiplicity. There is some evidence regarding gas-phase activation energies for H-stable hydrocarbon addition reactions (Payne & Stief 1976; Penzhorn & Darwent 1971; Scheer & Klein 1961; Daby, Niki, & Weinstock 1971; Cowfer et al. 1971). Based on the measured activation energy for H atom addition to acetylene (Payne & Stief 1976), we assume the activation energy for all hydrogenation reactions of the sort $C_nH_2 + H \rightarrow C_nH_3$ (involving C≡C "triple" bonds) to be 1210 K. Although there is evidence that the activation energy for addition to somewhat more saturated stable hydrocarbons (containing C=C "double" bonds, e.g., C_2H_4) is lower (≈ 750 K), such reactions are not included in the model, with the exception of $H + C_2H_4 \rightarrow C_2H_5$, because we only consider hydrocarbons through four hydrogen atoms when there are three or more carbon atoms. This is clearly an artificial constraint in the model; if acetylenic addition is efficient, addition to double bonds will be more so, since the activation energies are typically lower, and complete saturation to paraffins (C_nH_{2n+2}) may well be the outcome.

We have also included hydrogenation reactions to cyanopolyynes ($HC_{2n}CN$), which are assumed to have an activation energy of 1210 K in analogy to the $H + C_2H_2$ reaction. The

TABLE 2

SURFACE SPECIES CONSIDERED IN THIS WORK

H	FeH	HCN	HCCN	C_6H	H_3C_5N
C	CN	HNC	C_5	C_5H_2	HC_7N
N	CO	HCO	CH_4	C_4H_3	C_9N
O	NO	HOC	SiH_4	C_3H_4	C_9H
Na	CS	HNO	C_4H	C_2H_5	C_8H_2
Mg	SO	HCS	C_3H_2	HC_5N	C_7H_3
Si	C_3	OCN	C_2H_3	H_3C_3N	C_6H_4
S	O_3	OCS	HC_3N	C_8	H_2C_7N
Fe	C_2H	C_4	CH_2OH	C_7N	C_9H_2
H_2	N_2H	CH_3	CH_2CN	C_7H	C_8H_3
C_2	O_2H	NH_3	C_6	C_6H_2	C_7H_4
N_2	CH_2	SiH_3	C_5H	C_5H_3	H_3C_7N
O_2	NH_2	C_3N	C_5N	C_4H_4	HC_9N
CH	H_2O	C_3O	C_4H_2	C_2H_6	C_9H_3
NH	MgH_2	C_3H	C_3H_3	H_2C_5N	C_8H_4
OH	SiH_2	C_2H_2	C_2H_4	C_9	H_2C_9N
NaH	H_2S	N_2H_2	CH_3OH	C_8H	C_9H_4
MgH	C_2N	H_2O_2	CH_3CN	C_7H_2	H_3C_9N
SiH	CO_2	H_2CO	H_2C_3N	C_6H_3	
HS	SO_2	CHOH	C_7	C_5H_4	

TABLE 3

GRAIN SURFACE REACTIONS

Reactants		Products		kij (cm^3 s^{-1})	Ea (K)	Number		References
H	H	H2		3.88E+12	0	14	1	
H	C	CH		1.94E+12	0	14	2	AR
H	N	NH		1.94E+12	0	14	3	AR
H	O	OH		1.94E+12	0	14	4	AR
H	S	HS		1.94E+12	0	14	5	
H	SI	SIH		1.94E+12	0	14	6	
H	MG	MGH		1.94E+12	0	14	7	
H	NA	NAH		1.94E+12	0	14	8	
H	FE	FEH		1.94E+12	0	14	9	
H	CH	CH2		1.94E+12	0	14	10	AR
H	NH	NH2		1.94E+12	0	14	11	AR
H	OH	H2O		1.94E+12	0	14	12	AR
H	SIH	SIH2		1.94E+12	0	14	13	
H	HS	H2S		1.94E+12	0	14	14	
H	MGH	MGH2		1.94E+12	0	14	15	
H	C2	C2H		1.94E+12	0	14	16	AR
H	CN	HCN		1.94E+12	0	14	17	AR
H	CO	HCO		2.57E+06	1000	14	18	TH
H	CO	HOC		2.57E+06	1000	14	19	
H	NO	HNO		1.94E+12	0	14	20	AR
H	O2	O2H		1.51E+06	1200	14	21	TH
H	N2	N2H		1.51E+06	1200	14	22	
H	CS	HCS		5.15E+06	1000	14	23	
H	CH2	CH3		1.94E+12	0	14	24	AR
H	NH2	NH3		1.94E+12	0	14	25	AR
H	SIH2	SIH3		1.94E+12	0	14	26	
H	H2S	H2	HS	1.31E+07	860	14	27	TH
H	C2H	C2H2		1.94E+12	0	14	28	AR
H	HCO	H2CO		1.94E+12	0	14	29	AR
H	HOC	CHOH		1.94E+12	0	14	30	AR
H	O2H	H2O2		1.94E+12	0	14	31	AR
H	C3	C3H		1.94E+12	0	14	32	
H	O3	O2	OH	3.53E+08	450	14	33	TH
H	C2N	HCCN		1.94E+12	0	14	34	AR
H	N2H	N2H2		1.94E+12	0	14	35	AR
H	CH3	CH4		1.94E+12	0	14	36	AR
H	SIH3	SIH4		1.94E+12	0	14	37	
H	H2CO	HCO	H2	5.06E+04	1850	14	38	TH
H	CHOH	CH2OH		1.94E+12	0	14	39	AR
H	H2O2	H2O	OH	4.90E+05	1400	14	40	TH
H	N2H2	N2H	H2	6.20E+07	650	14	41	TH
H	HCCN	C2H2N		1.94E+12	0	14	42	AR
H	C2H2	C2H3		1.43E+06	1210	14	43	
H	C3H	C3H2		1.94E+12	0	14	44	AR
H	C4	C4H		1.94E+12	0	14	45	
H	C3N	HC3N		1.94E+12	0	14	46	
H	C2H3	C2H4		1.94E+12	0	14	47	AR
H	C3H2	C3H3		1.43E+06	1210	14	48	
H	CH2OH	CH3OH		1.94E+12	0	14	49	AR
H	C2H2N	C2H3N		1.94E+12	0	14	50	AR
H	HC3N	C3H2N		1.43E+06	1210	14	51	
H	C4H	C4H2		1.94E+12	0	14	52	AR
H	C5	C5H		1.94E+12	0	14	53	
H	C2H4	C2H5		2.88E+07	750	14	54	
H	C3H3	C3H4		1.94E+12	0	14	55	AR
H	C4H2	C4H3		1.43E+06	1210	14	56	
H	C5H	C5H2		1.94E+12	0	14	57	
H	C5N	HC5N		1.94E+12	0	14	58	
H	C6	C6H		1.94E+12	0	14	59	
H	C3H2N	C3H3N		1.94E+12	0	14	60	
H	C2H5	C2H6		1.94E+12	0	14	61	
H	C4H3	C4H4		1.94E+12	0	14	62	
H	C5H2	C5H3		1.43E+06	1210	14	63	
H	C6H	C6H2		1.94E+12	0	14	64	
H	C7	C7H		1.94E+12	0	14	65	
H	HC5N	C5H2N		1.43E+06	1210	14	66	
H	C5H3	C5H4		1.94E+12	0	14	67	
H	C6H2	C6H3		1.43E+06	1210	14	68	
H	C7H	C7H2		1.94E+12	0	14	69	
H	C7N	HC7N		1.94E+12	0	14	70	
H	C8	C8H		1.94E+12	0	14	71	
H	C5H2N	C5H3N		1.94E+12	0	14	72	
H	C6H3	C6H4		1.94E+12	0	14	73	
H	C7H2	C7H3		1.43E+06	1210	14	74	
H	C8H	C8H2		1.94E+12	0	14	75	
H	C9	C9H		1.94E+12	0	14	76	
H	HC7N	C7H2N		1.43E+06	1210	14	77	
H	C7H3	C7H4		1.94E+12	0	14	78	
H	C8H2	C8H3		1.43E+06	1210	14	79	
H	C9H	C9H2		1.94E+12	0	14	80	
H	C9N	HC9N		1.94E+12	0	14	81	
H	C7H2N	C7H3N		1.94E+12	0	14	82	
H	C8H3	C8H4		1.94E+12	0	14	83	
H	C9H2	C9H3		1.43E+06	1210	14	84	
H	HC9N	C9H2N		1.43E+06	1210	14	85	
H	C9H3	C9H4		1.94E+12	0	14	86	
H	C9H2N	C9H3N		1.94E+12	0	14	87	
H2	OH	H2O	H	2.20E-02	2600	14	88	TH
C	C	C2		3.71E+03	0	14	89	AR

TABLE 3—*Continued*

Reactants		Products		kij (cm^3 s^{-1})	Ea (K)	Number	References
C	N	CN		3.57E+03	0	14 90	AR
C	O	CO		3.46E+03	0	14 91	AR
C	S	CS		1.86E+03	0	14 92	
C	CH	C2H		1.33E+05	0	14 93	AR
C	NH	HNC		5.28E+05	0	14 94	AR
C	OH	HOC		9.30E+02	0	14 95	AR
C	OH	CO	H	9.30E+02	0	14 96	
C	C2	C3		1.86E+03	0	14 97	AR
C	CN	C2N		1.86E+03	0	14 98	AR
C	NO	OCN		1.86E+03	0	14 99	AR
C	O2	CO	O	1.86E+03	0	14 100	AR
C	CH2	C2H2		1.86E+03	0	14 101	AR
C	NH2	HNC	H	2.16E+03	0	14 102	
C	C3	C4		1.86E+03	0	14 103	
C	C2H	C3H		1.86E+03	0	14 104	AR
C	C2N	C3N		1.86E+03	0	14 105	
C	OCN	CO	CN	1.86E+03	0	14 107	MD
C	CH3	C2H3		1.86E+03	0	14 108	AR
C	C3H	C4H		1.86E+03	0	14 109	AR
C	C4	C5		1.86E+03	0	14 110	
C	C5	C6		1.86E+03	0	14 111	
C	C2H3	C3H3		1.86E+03	0	14 112	AR
C	C6	C7		1.86E+03	0	14 113	
C	C7	C8		1.86E+03	0	14 114	
C	C8	C9		1.86E+03	0	14 115	
N	N	N2		3.43E+03	0	14 116	AR
N	O	NO		3.32E+03	0	14 117	AR
N	CH	HCN		1.33E+05	0	14 118	AR
N	NH	N2H		5.28E+05	0	14 119	AR
N	C2	C2N		1.72E+03	0	14 120	AR
N	NH2	N2H2		2.02E+03	0	14 121	AR
N	C3	C3N		1.72E+03	0	14 122	
N	C3H	HC3N		1.72E+03	0	14 123	
N	C5	C5N		1.72E+03	0	14 124	
N	C5H	HC5N		1.72E+03	0	14 125	
N	C7	C7N		1.72E+03	0	14 126	
N	C7H	HC7N		1.72E+03	0	14 127	
N	C9	C9N		1.72E+03	0	14 128	
N	C9H	HC9N		1.72E+03	0	14 129	
O	O	O2		3.21E+03	0	14 130	AR
O	S	SO		1.61E+03	0	14 131	TH
O	CH	HCO		1.33E+05	0	14 132	AR
O	NH	HNO		5.28E+05	0	14 133	AR
O	OH	O2H		1.61E+03	0	14 134	AR
O	CN	OCN		1.61E+03	0	14 135	AR
O	O2	O3		1.61E+03	0	14 136	TH, AR
O	CO	CO2		1.61E+03	0	14 137	TH
O	CS	OCS		1.61E+03	0	14 138	TH
O	SO	SO2		1.61E+03	0	14 139	TH
O	HCO	CO2	H	1.61E+03	0	14 140	M
O	CH2	H2CO		1.61E+03	0	14 141	AR
O	C3	C3O		1.61E+03	0	14 142	
O	CH3	CH2OH		1.61E+03	0	14 143	AR, B
CH	CH	C2H2		2.63E+05	0	14 144	AR
CH	OH	CHOH		1.31E+05	0	14 145	AR
CH	C2	C3H		1.31E+05	0	14 146	AR
CH	C2H	C3H2		1.31E+05	0	14 147	AR
CH	HNO	NO	CH2	1.31E+05	0	14 148	M
CH	CH3	C2H4		1.31E+05	0	14 149	AR
CH	C3	C4H		1.31E+05	0	14 150	
CH	C4	C5H		1.31E+05	0	14 151	
CH	C5	C6H		1.31E+05	0	14 152	
CH	C6	C7H		1.31E+05	0	14 153	
CH	C7	C8H		1.31E+05	0	14 154	
CH	C8	C9H		1.31E+05	0	14 155	
OH	OH	H2O2		3.97E-03	0	14 156	AR
OH	CH2	CH2OH		1.71E+01	0	14 157	AR

NOTES.—aE ± b means $a \times 10^{\pm b}$. Ea = Activation energy.

REFERENCES.—AR: Allen & Robinson 1977; TH: Tielens & Hagen 1982; M: Mitchell 1984; MD: Mitchell & Deveau 1983; B: Brown 1990.

radical species ($H_2C_{2n}CN$) formed by these reactions will then add another hydrogen atom without activation energy to form species of the type $H_3C_{2n}CN$ (or structural isomers), and we once again assume arbitrarily that hydrogenation does not proceed any further.

Finally, two reactions in the set merit special mention. The reaction between CO and O to form CO_2 has been utilized in past treatments (TH) but recently has been measured to be slow in the absence of irradiation (Grim & d'Hendecourt 1986; Breukers 1991). We have run models with and without this reaction to ascertain its importance in regulating the CO–CO_2 balance on grain surfaces. We have introduced the reaction $H + N_2 \rightarrow HN_2$ and assumed it to have an activation energy of 1200 K. The existence of HN_2 in the gas phase is controversial. *Ab initio* calculations indicate that it possesses a local minimum in its potential energy surface but that the minimum lies above the energy of the $H + N_2$ reactants (Schatz, Koizumi, & Lendvay 1991).

3. RESULTS

The gas-grain model was calculated for three different initial conditions, common to which is the assumption that the grains are without mantles. In all cases, $n = n(H) + 2n(H_2) = 2 \times 10^4$ cm^{-3}, $T_d = T_k = 10$ K, and visual extinction $A_V = 500$. In model A, the initial gas-phase composition is given by the *steady state* abundances of HL2. This represents the so-called hydrogen-poor case (TA), and the calculated surface abundances can be compared with those obtained by TH, who used similar initial conditions. In model B the gas phase is initially atomic and neutral. The initial conditions for model C are those usually utilized in gas-phase pseudo–time-dependent models and represent the denser portions of diffuse clouds; the hydrogen is molecular, and carbon, sulfur, and metals are atomic and singly ionized. Finally, a fourth model, model D, was run. Model D is the same as model C, except that the reaction between CO and O to form CO_2 is eliminated. The gas-phase species in each of the models at $t = 0$ are listed in Table 4, which also shows the dominant molecules on the grain surfaces at the chemically useful ("early") time of 3×10^5 yr as well as the final time calculated ($t = 1 \times 10^7$ yr). The abundances of the dominant surface molecules are listed as a percentage by number of all atoms and molecules on the surface. The time evolution of important gaseous and surface species in each model is shown in Figures 1–4, for models A–D, respectively. The abundances are plotted as gaseous or surface concentrations divided by $n/2 = n(H_2) + 0.5n(H)$; although $n/2$ strictly refers to the total abundance of hydrogen, it is approximately equal to the sum of the gaseous species only. The surface fractional abundances can be converted into numbers of molecules per grain by multiplication by $n/2$ and division by the grain number density n_d. The time evolution of surface hydrocarbons in models B and C is shown in Figures 5 and 6, while Figure 7 contains the time evolution of surface

TABLE 4

INITIAL CONDITIONS AND GRAIN-SURFACE COMPOSITION

A. INITIAL CONDITIONS

Species	Model A	Model B	Model C	Model D[a]
Hydrogen	H_2	H	H_2	H_2
O, C, S, Si	Steady state molecular abundances[b]	Neutral atomic	O neutral, C, S, Si ionized	O neutral, C, S, Si ionized
Metals	Steady state	Neutral atomic	[c]	[c]

B. SURFACE COMPOSITION (% by molecular number)[d]

	Model A		Model B		Model C		Model D	
Species	3(5) yr	1(7) yr	3(5) yr	1(7) yr	3(5) yr	1(7) yr	3(5) yr	1(7) yr
H_2	3	1	1	1	3	1	2	1
CO	10	...	...	...	...	...	6	...
N_2	5	...	...	...	2	...	2	...
O_2	13	...	...	...	...	...	...	...
H_2O	19	48	60	55	39	40	52	53
CO_2	14	11	1	7	43	37	11	6
HNO	...	...	...	...	3	2	3	2
HCN	...	...	...	1	2	1	1	1
H_2CO	13	16	5	7	...	5	4	12
NH_3	...	...	9	8	...	...	...	...
N_2H_2	3	6	...	1	3	6	2	5
H_2O_2	7	2	...	...	...	...	...	...
CH_4	...	...	18	13	1	2	1	1
CH_3OH	13	16	5	7	...	5	15	18
CH_3CN	...	...	...	...	1	...	...	...

[a] Differs from model C only in the exclusion of the $CO + O \rightarrow CO_2$ reaction.
[b] Steady state abundances taken from the work of Herbst & Leung 1989.
[c] Singly ionized atoms.
[d] Abundances ≥1% shown.

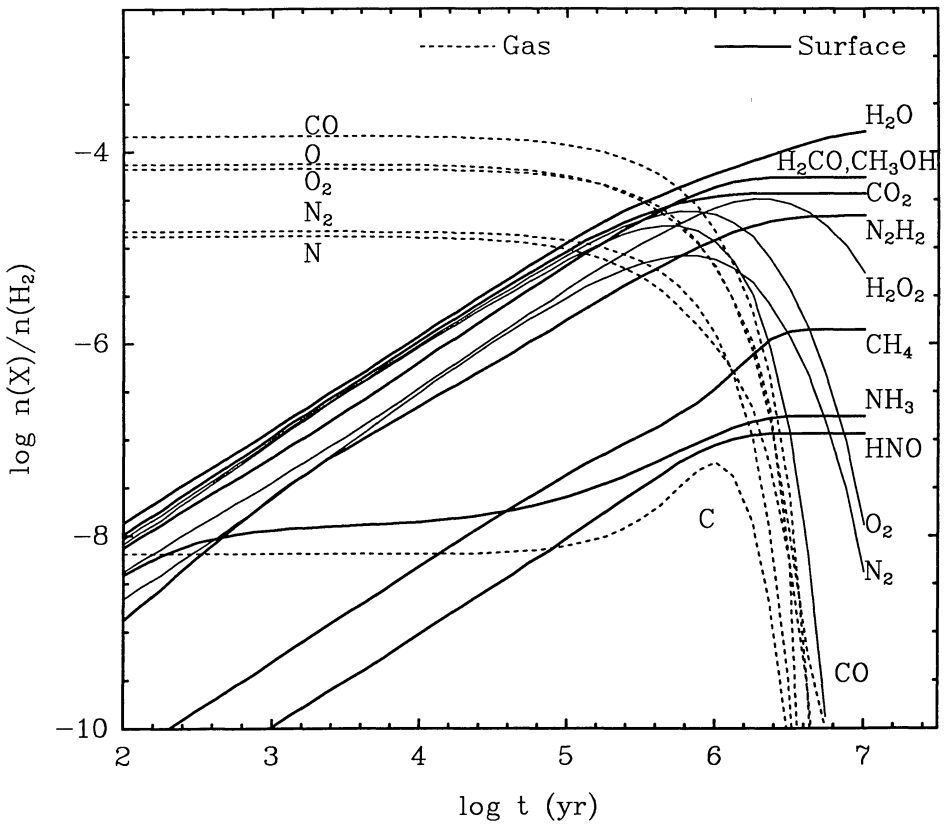

FIG. 1.—Time evolution of the fractional abundances of important gas-phase (*dashed line*) and surface (*solid line*) species for model A. The fractional abundances are defined with respect to $n/2 \approx n(H_2)$.

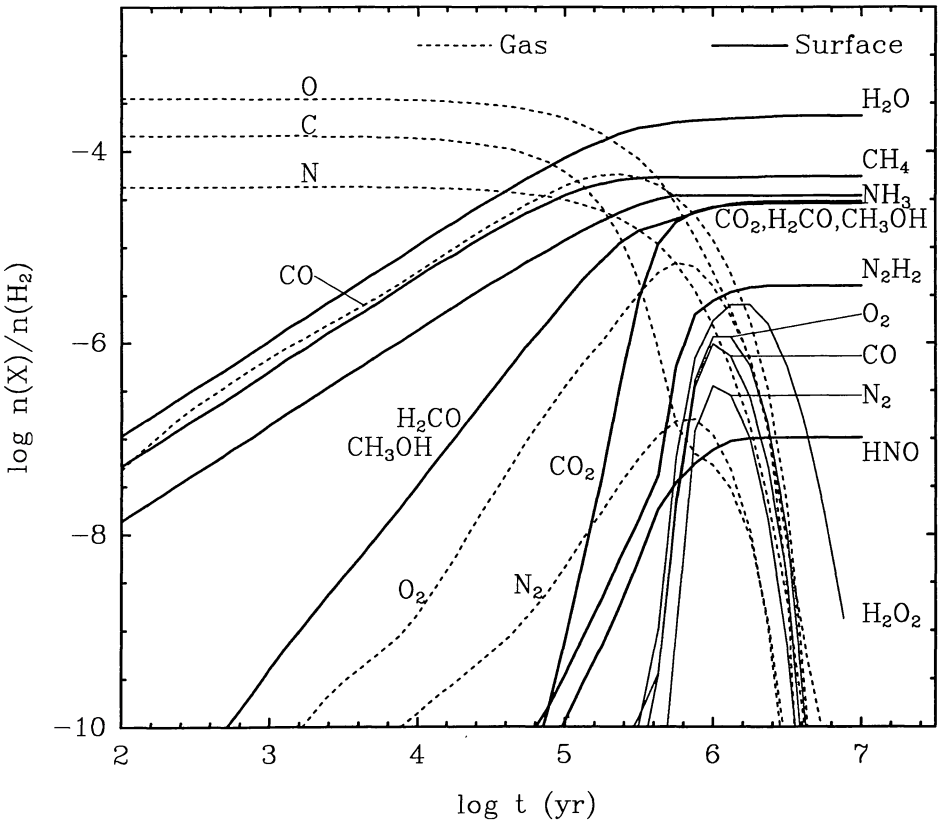

FIG. 2.—Time evolution of the fractional abundances of important gas-phase (*dashed line*) and surface (*solid line*) species for model B. The fractional abundances are defined with respect to $n/2$, which here differs appreciably from $n(H_2)$ at early stages.

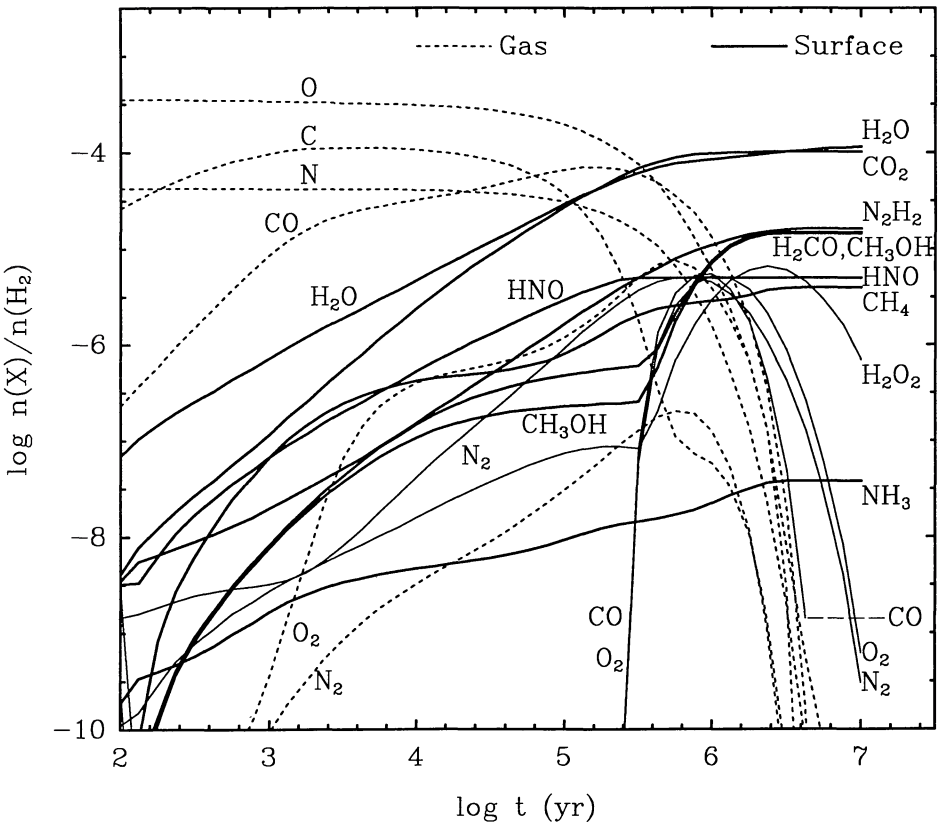

FIG. 3.—Time evolution of the fractional abundances of important gas-phase (*dashed line*) and surface (*solid line*) species for model C. The fractional abundances are defined with respect to $n/2 \approx n(H_2)$.

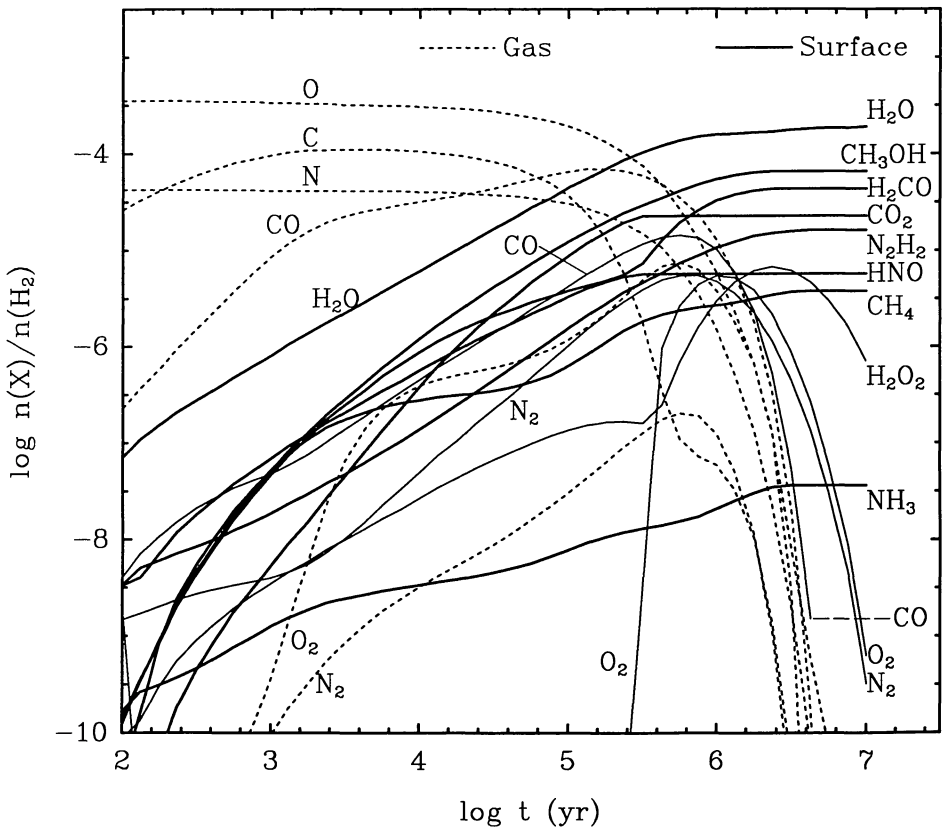

FIG. 4.—Time evolution of the fractional abundances of important gas-phase (*dashed line*) and surface (*solid line*) species for model D. The fractional abundances are defined with respect to $n/2 \approx n(H_2)$.

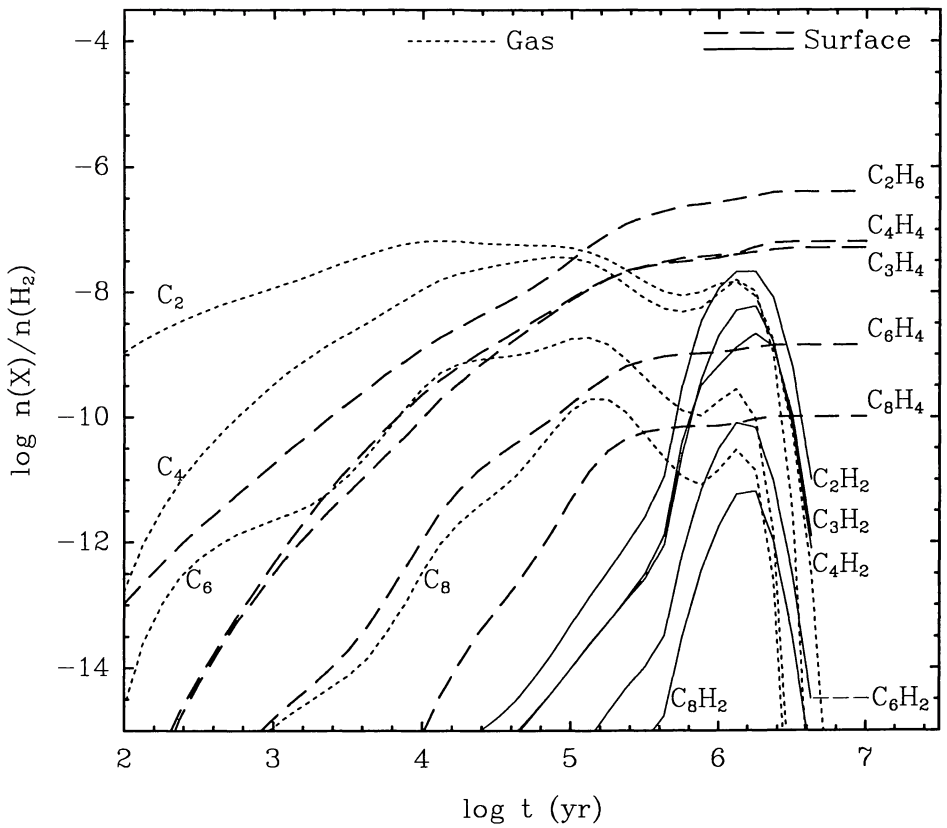

FIG. 5.—Time evolution of fractional abundances of hydrocarbons in model B. Bare carbon clusters in the gas are depicted by short dashes, more saturated surface species by long dashes, and less saturated surface species by solid lines.

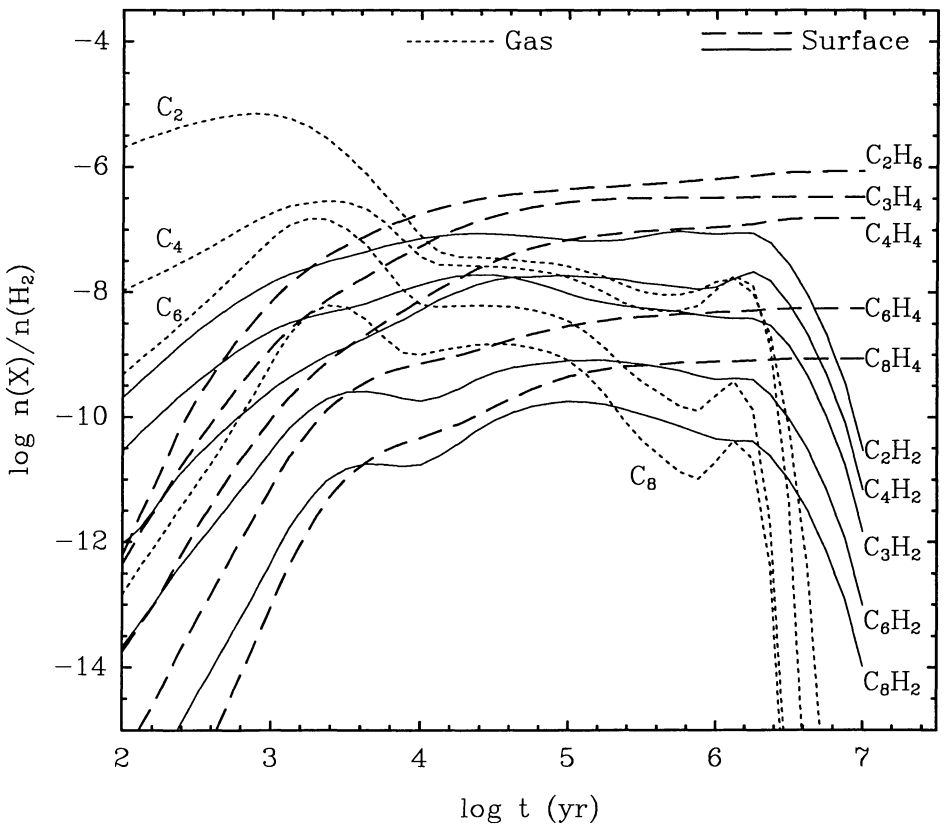

FIG. 6.—Time evolution of fractional abundances of hydrocarbons in model C. Bare carbon clusters in the gas are depicted by short dashes, more saturated surface species by long dashes, and less saturated surface species by solid lines.

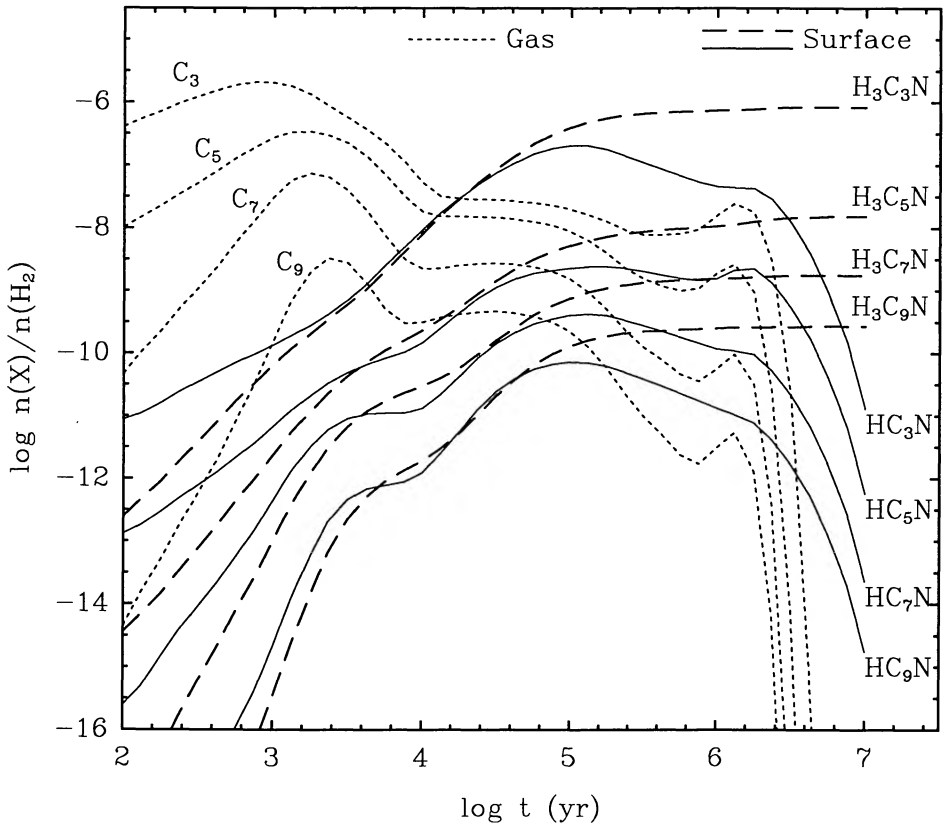

FIG. 7.—Time evolution of gas-phase carbon clusters and surface organo-nitrogen species in model C. Surface cyanopolyynes are depicted by solid lines, whereas more saturated surface species are depicted by long dashes.

organo-nitrogen species in model C. Finally, Tables 5, 6, 7, and 8 give fractional abundances with respect to $n/2$ from models A, B, C, and D, respectively, for all neutral species (in the gas and on grain surfaces) and selected gaseous ions at times from 1×10^5 through 1×10^7 yr.

The chemical pathways leading to the dominant and complex molecules found on grain surfaces, as well as the time dependence of their abundances, are discussed below. Those readers not interested in these details can profitably skip to § 4, where a small subset of the results is compared with both observation and other grain and gas-grain models.

3.1. *Model A*

In this model, the gas phase starts with steady state abundances, and the dominant steady state species (CO, O_2, O, N_2, and N) accrete slowly onto the grain surfaces, as can be seen in Figure 1, which shows the gradual decline in their gas-phase abundances. The gas-phase chemistry occurring during this accretion stage is not altogether simple, and, as can be seen in Table 5, some complex molecules actually show small peaks in their abundances before total accretion of heavy molecules occurs. Surface abundances build up slowly and begin to dominate gas-phase abundances at a time of approximately 10^6 yr. The initial gaseous atomic hydrogen abundance is low, and, as it accretes, it is not able to hydrogenate all atomic species efficiently because heavier atoms, despite their lower surface reaction rate coefficients, react competitively. A glance at the final surface abundances in Figure 1 or Table 4 shows that only atomic oxygen is efficiently converted into the simple saturated form of water.

The H atom abundance on the grain surface is kept quite low by a catalytic process involving N_2, which is depleted in our model by hydrogenation to N_2H. This radical is also formed via the NH + N reaction, as discussed by TH, who were the first to consider catalytic cycles of this type. The N_2H radical is hydrogenated by H atoms to form N_2H_2, which itself can react slowly with H atoms via the abstraction process (TH) $N_2H_2 + H \rightarrow N_2H + H_2$ which reforms N_2H as it depletes H. The re-formed N_2H can then consume another H atom. Since N_2 is continually accreting in this model, the H atom surface abundance is minimized and hydrogenation of other species such as N and C atoms is suppressed. The dominant nitrogen-containing species on the surface becomes N_2H_2. Ammonia and methane on grain surfaces reach asymptotic fractional abundances of only 2×10^{-7} and 1×10^{-6}, respectively. The hydrogenation of O atoms to produce OH radicals and especially water occurs through a convoluted but efficient process involving ozone production, as first pointed out by TH. Due to accretion, there is a relatively high abundance of CO on the

surface from $t = 10^5$ to $t = 10^6$ yr, which is eventually depleted via reaction with O atoms to form CO_2 and by hydrogenation with H to form H_2CO via the pathway CO → HCO → H_2CO, and methanol via the pathway CO → HOC → HOCH → $HOCH_2$ → CH_3OH. Both formaldehyde and methanol achieve very large abundances and are second behind water as the dominant species on grain surfaces. Note that we have arbitrarily used HOC as the intermediary to methanol production; one could just as easily assume that H atom addition to HCO leads to HOCH on a certain fraction of collisions.

Complex molecule abundances (e.g., hydrocarbons and cyanopolyynes) are low in the steady state gas-phase results utilized as initial conditions. Although some of these abundances increase in the gas phase as the gas-grain chemistry evolves, large abundances are not achieved on grain surfaces, owing primarily to the small abundance of atomic carbon, which is needed to produce complex molecules on grain surfaces.

3.2. *Model B*

This model calculation starts from a completely atomic gas. Detailed results are shown in Table 6, while the time dependence of the abundances of important species is shown in Figure 2. The gaseous atomic hydrogen is converted to gaseous molecular hydrogen in $\approx 10^6$ yr by accretion, surface reaction, and thermal evaporation. The concentration of gaseous atomic hydrogen is reduced to its steady state value of 1 cm^{-3} at 10^6 yr. Interestingly, the conversion of atomic to molecular hydrogen on grain surfaces occurs not only via the standard H + H → H_2 surface recombination but by catalytic cycles as well (TH). At early times (10^3–10^5 yr) after a reasonable supply of sulfur atoms has accreted onto the grains, a significant fraction of the conversion occurs via the catalytic loop HS + H → H_2S, H_2S + H → HS + H_2, whereas by 1×10^5 yr, when sufficient surface CO has been built up, the analogous loop HCO + H → H_2CO, H_2CO + H → HCO + H_2 also occurs, in addition to the similar HN_2 loop discussed in § 3.1. Both loops occur despite the existence of activation energy in the second (hydrogen abstraction) reaction.

The gas-phase chemistry initially evolves in a manner not very different from that in purely gas-phase pseudo–time-dependent models. Since the initial gas is atomic, the so-called early time, at which complex molecules reach their maximum abundances (HL1; HL2), occurs somewhat later than the standard 1×10^5 yr (see Table 6), a fact that has been shown in previous work (Brown & Charnley 1991; Pineau des Forêts et al. 1991). At $t = 1 \times 10^5$ yr, about half of the carbon has already been converted into CO, whereas relatively little O_2 has been formed. The peak organic gas-phase abundances occur at $t \approx 3 \times 10^5$ yr; in general these are not as high as peak abundances obtained with the starting conditions in model C and are too low to explain observations in TMC-1. The gas-phase O_2 fractional abundance peaks at under 10^{-5} at $t = 6 \times 10^5$ yr. After this time, all gas-phase abundances decline due to grain accretion.

As the surface chemistry evolves, H atom hydrogenation plays a dominant role in the production of the saturated simple species H_2O, NH_3, CH_4, and H_2S from accreted heavy atoms. Water, methane, and ammonia become the dominant surface molecular species, as can be seen in Figure 2. By 1×10^5 yr, these three surface molecules contain much of the overall elemental abundances of oxygen, nitrogen, and carbon, respectively. This result is in line with previous models of "H-rich" surface chemistry (e.g., TA; Brown et al. 1988). After 3×10^5 yr, as the gas becomes rich in molecules, especially H_2 and CO, the accreting gas resembles that found in model A, at least for the simpler species. The surface chemistry becomes relatively poor in atomic hydrogen, and CO_2, H_2CO, CH_3OH, and N_2H_2 are formed efficiently.

Hydrocarbon development proceeds more efficiently in model B than in model A, owing to the high abundance of neutral atomic C in the gas at various epochs. The abundances of various carbon clusters in the gas and hydrocarbons on the grain surface are shown in Figure 5 as a function of time. The initial synthesis occurs in the gas, where carbon clusters and unsaturated species such as C_nH are produced relatively quickly compared with other complex species (3×10^4–1×10^5 yr) via ion-molecule pathways and accrete onto the grain surfaces, where the dominant process is hydrogenation. Further synthesis of more complex species via C atom addition on the grain surface is a minor process, because of the relative shortage of surface C. The saturated grain species gradually increase in abundance and reach their asymptotic values at $\approx 3 \times 10^5$–1×10^6 yr. In general, the more complex the hydrocarbon, the lower the abundance (see Fig. 5 or Table 6). At a time $t = 3 \times 10^5$ yr, the abundances of the saturated hydrocarbons on the grain surfaces are roughly equivalent to the abundances of the dominant unsaturated counterparts in the gas. For example, the total fractional abundance of eight–carbon-atom hydrocarbons (consisting of C_8, C_8H, and C_8H_2) in the gas is 8.5×10^{-11}, whereas the total surface fractional abundance is 5.8×10^{-11}, pretty much all in the form of C_8H_4. At later times, however, the gas-phase abundances decrease strongly, whereas the saturated surface species, with no destruction pathways in our model, remain at their asymptotic values.

As can be seen in Figure 5, there is a secondary, later maximum for the abundances of the gaseous carbon cluster species, at approximately 10^6 yr. This is caused by an increase in the C abundance, which in turn is caused by a decrease in the O_2 abundance due to accretion. (Oxygen is the main destroyer of C.) As these newly formed cluster species accrete, grain surface chemistry is now atomic-hydrogen–poor and saturation occurs slowly enough so that acetylenic (C_nH_2) hydrocarbons on the surface reach peaks in abundance before declining. The dominant pathways to hydrocarbon formation on grain surfaces at $t = 1 \times 10^6$ yr are shown in Figure 8. It can be seen that, at this time, accretion of carbon clusters formed in the gas is once more the driving force in hydrocarbon synthesis, with the surface contribution mainly slow hydrogenation.

Cyanopolyynes are formed on grain surfaces in model B only during the secondary stage of hydrocarbon formation (between 1 and 3×10^6 yr) because in the earlier stage there is enough atomic hydrogen so that hydrogenation of hydrocarbons dominates. *They are thus not present at early times usually used to compare gas-phase model calculations with observation.* At the later stage, however, accreted carbon clusters and unsaturated hydrocarbons have a large chance of adding an atomic nitrogen to form cyanopolyynes and cyanopolyyne radicals. This is also illustrated in Figure 8 for a time of 1×10^6 yr. Once produced, the cyanopolyynes are saturated gradually,

TABLE 5

GAS AND SURFACE ABUNDANCES FOR MODEL A EXPRESSED AS A FRACTION OF TOTAL H_2 + 0.5H

t(yr)	1.0E+05		3.2E+05		1.0E+06		1.0E+07
Species	Gas	Surface	Gas	Surface	Gas	Surface	Surface
H	1.0E-04	1.1E-23	1.0E-04	4.1E-24	1.0E-04	2.2E-24	1.7E-24
*HE	2.8E-01	1.5E-21	2.8E-01	1.5E-21	2.8E-01	1.5E-21	1.5E-21
C	7.7E-09	5.5E-24	1.5E-08	4.6E-24	5.8E-08	1.6E-23	2.1E-30
N	9.5E-06	1.2E-13	4.9E-06	8.4E-14	9.0E-07	3.5E-14	7.0E-24
O	5.5E-05	2.1E-20	3.0E-05	5.2E-21	6.3E-06	1.1E-21	9.3E-29
NA	1.0E-09	3.9E-16	8.6E-10	8.6E-16	5.0E-10	9.1E-16	3.4E-17
MG	3.8E-09	1.4E-15	3.1E-09	3.1E-15	1.9E-09	3.4E-15	1.1E-16
SI	1.2E-08	4.2E-15	7.2E-09	6.5E-15	1.4E-09	2.3E-15	2.4E-21
S	5.4E-08	1.7E-14	5.2E-08	4.4E-14	2.1E-08	3.2E-14	1.4E-18
FE	1.2E-09	3.0E-16	9.8E-10	6.3E-16	4.3E-10	5.1E-16	3.5E-17
H2	1.0E+00	4.0E-06	1.0E+00	4.0E-06	1.0E+00	4.0E-06	4.0E-06
CH	3.6E-11	3.1E-25	7.9E-11	2.1E-25	8.0E-10	7.4E-25	3.6E-33
NH	1.1E-09	3.9E-17	9.4E-10	1.5E-17	4.9E-10	8.4E-18	7.0E-24
OH	3.7E-08	3.3E-15	5.7E-08	2.0E-15	1.3E-07	7.8E-16	5.0E-17
C2	3.7E-10	1.3E-17	1.4E-09	7.0E-17	1.6E-08	1.9E-15	1.6E-33
NAH	1.9E-13	2.8E-10	1.4E-13	7.8E-10	5.1E-14	1.9E-09	3.6E-09
MGH	4.6E-13	1.4E-15	2.5E-13	3.1E-15	2.5E-14	3.4E-15	1.1E-16
FEH		2.1E-10		5.9E-10		1.3E-09	2.3E-09
CN	5.0E-09	1.8E-15	9.7E-09	9.1E-15	1.0E-08	1.7E-14	1.5E-23
N2	1.2E-05	3.0E-06	7.1E-06	6.8E-06	1.2E-06	7.4E-06	4.2E-09
CO	1.2E-04	7.3E-06	7.1E-05	1.5E-05	1.5E-05	1.1E-05	1.1E-15
SIH	2.6E-10	4.3E-15	3.4E-10	6.8E-15	2.5E-10	2.7E-15	2.6E-21
NO	4.3E-08	1.4E-14	4.8E-08	4.2E-14	2.3E-08	3.9E-14	1.7E-23
O2	5.3E-05	8.3E-06	3.3E-05	1.9E-05	6.0E-06	2.2E-05	1.3E-08
HS	1.6E-11	9.4E-14	2.6E-11	2.9E-13	3.1E-11	6.4E-13	7.6E-13
*SIC	2.6E-12	4.2E-13	4.6E-12	1.9E-12	4.4E-12	9.3E-12	1.2E-11
*SIO	4.7E-10	9.9E-11	2.5E-10	2.4E-10	2.5E-11	3.6E-10	3.7E-10
CS	1.1E-08	5.4E-10	6.1E-09	1.1E-09	5.9E-10	5.1E-10	1.5E-19
*NS	4.2E-11	8.7E-12	2.3E-11	2.1E-11	2.0E-12	3.2E-11	3.3E-11
SO	1.4E-08	1.3E-09	6.0E-09	2.8E-09	2.1E-10	2.5E-09	1.9E-09
*SIS	1.6E-11	3.0E-12	5.6E-12	6.3E-12	7.7E-14	7.8E-12	7.8E-12
CH2	9.1E-10	4.6E-16	1.6E-09	2.2E-15	4.6E-09	1.3E-14	8.6E-23
NH2	2.6E-08	9.8E-16	2.8E-08	1.5E-15	1.8E-08	2.3E-15	7.0E-24
H2O	3.9E-07	1.1E-05	3.0E-07	2.9E-05	2.0E-07	5.9E-05	1.6E-04
SIH2		4.3E-15		6.8E-15		2.7E-15	2.6E-21
MGH2		9.9E-10		2.8E-09		7.0E-09	1.3E-08
C2H	2.8E-10	1.2E-16	4.3E-10	4.8E-16	2.2E-09	5.8E-15	1.7E-33
N2H		5.9E-11		1.6E-10		3.9E-10	6.8E-10
O2H		6.5E-12		1.5E-11		1.7E-11	1.0E-14
HCN	1.7E-09	1.4E-09	2.6E-09	6.1E-09	3.1E-09	3.2E-08	4.6E-08

t(yr)	1.0E+05		3.2E+05		1.0E+06		1.0E+07
Species	Gas	Surface	Gas	Surface	Gas	Surface	Surface
HNC	1.7E-09	3.8E-10	2.6E-09	1.4E-09	3.1E-09	6.9E-09	1.0E-08
HCO	8.9E-11	9.9E-12	1.2E-10	2.1E-11	3.8E-10	1.6E-11	1.4E-12
HOC		9.7E-12		2.0E-11		1.5E-11	1.4E-21
HCS		9.6E-10		2.8E-09		5.6E-09	6.3E-09
HNO	1.3E-11	9.3E-09	6.8E-12	3.1E-08	7.6E-13	8.7E-08	1.2E-07
H2S	2.1E-10	1.1E-08	2.1E-10	3.6E-08	8.6E-11	9.0E-08	1.1E-07
C3	7.6E-11	2.2E-18	2.5E-10	1.0E-17	9.0E-09	8.8E-16	4.8E-39
O3		7.3E-08		1.1E-07		5.1E-08	3.3E-18
C2N	1.3E-10	1.6E-16	1.4E-10	1.4E-15	8.9E-11	2.7E-14	1.9E-38
*NAOH	1.2E-14	2.6E-15	6.1E-15	6.2E-15	8.9E-16	9.6E-15	1.0E-14
OCN	1.3E-08	2.6E-09	9.3E-09	7.0E-09	8.1E-10	1.3E-08	1.3E-08
CO2	7.7E-08	9.2E-06	4.5E-08	2.2E-05	4.8E-09	3.4E-05	3.6E-05
OCS	5.0E-08	9.8E-09	2.3E-08	2.3E-08	7.5E-10	3.1E-08	3.1E-08
SO2	3.6E-09	2.3E-09	8.5E-10	5.2E-09	5.9E-12	7.7E-09	8.4E-09
CH3	3.2E-10	6.2E-16	9.9E-10	3.4E-15	2.2E-08	6.3E-14	2.1E-22
NH3	3.6E-08	2.5E-08	3.6E-08	4.9E-08	2.2E-08	1.1E-07	1.7E-07
SIH3		4.3E-15		6.8E-15		2.7E-15	2.6E-21
C2H2	7.4E-09	1.3E-09	6.6E-09	3.6E-09	2.6E-08	2.1E-08	1.4E-10
N2H2		1.8E-06		5.0E-06		1.2E-05	2.1E-05
H2O2		3.7E-06		1.1E-05		2.6E-05	5.4E-06
H2CO	2.5E-09	6.6E-06	3.4E-09	1.9E-05	7.1E-09	4.2E-05	5.4E-05
CHOH		9.7E-12		2.0E-11		1.5E-11	1.4E-21
HCCN		1.6E-16		1.4E-15		2.7E-14	1.9E-38
C3H	9.7E-11	3.0E-18	1.4E-10	6.5E-18	8.6E-10	1.4E-16	5.2E-39
*H2CS	4.6E-11	9.5E-12	2.4E-11	2.2E-11	8.9E-12	3.9E-11	4.8E-11
C4	2.1E-11	5.6E-18	8.9E-11	6.2E-17	5.1E-09	6.6E-15	0.0E+00
C3N	1.1E-10	5.1E-17	2.1E-10	3.3E-16	5.7E-10	1.3E-14	3.5E-36
C3O	4.8E-12	8.1E-13	4.8E-12	2.5E-12	3.3E-12	7.7E-12	9.8E-12
CH4	1.2E-07	4.3E-08	9.0E-08	1.1E-07	1.2E-07	3.4E-07	1.4E-06
SIH4		3.1E-09		7.9E-09		1.4E-08	1.6E-08
C2H3	5.1E-10	1.2E-15	6.8E-10	3.3E-15	3.4E-09	2.1E-14	1.0E-16
*CH3N	2.2E-11	5.1E-12	2.6E-11	1.7E-11	2.6E-11	6.1E-11	9.3E-11
C3H2	1.2E-10	1.8E-11	1.9E-10	6.2E-11	1.2E-09	6.8E-10	5.0E-12
C2H2N	6.1E-11	1.8E-16	3.0E-11	1.4E-15	1.4E-11	2.7E-14	1.9E-38
*C2H2O	1.2E-10	2.6E-11	8.2E-11	6.5E-11	5.4E-11	1.5E-10	1.9E-10
*CH2O2	1.3E-09	2.8E-10	7.0E-10	6.5E-10	1.0E-10	1.0E-09	1.1E-09
CH2OH		9.7E-12		2.0E-11		1.5E-11	1.4E-21
C4H	4.8E-11	1.8E-17	9.5E-11	1.3E-16	1.0E-09	7.8E-15	0.0E+00
HC3N	1.4E-10	4.8E-11	1.9E-10	2.1E-10	3.9E-10	4.5E-09	5.1E-11
C5	1.5E-12	3.4E-20	7.5E-12	2.4E-19	7.1E-10	5.4E-17	0.0E+00
*C4N	3.5E-13	5.1E-14	6.6E-13	2.1E-13	5.7E-12	3.2E-12	1.0E-11
C2H4	5.0E-12	7.2E-11	3.2E-12	2.0E-10	1.4E-11	1.3E-09	7.1E-12
CH3OH	1.1E-11	6.6E-06	1.1E-11	1.9E-05	1.0E-11	4.2E-05	5.4E-05
C3H3	4.0E-13	1.4E-17	3.3E-13	4.6E-17	1.5E-12	5.0E-16	3.7E-18
C2H3N	5.9E-13	9.6E-11	1.1E-12	5.5E-10	2.0E-12	1.3E-08	4.6E-08
C3H2N		3.5E-17		1.5E-16		3.3E-15	3.8E-17

TABLE 5—*Continued*

t(yr)	1.0E+05		3.2E+05		1.0E+06		1.0E+07
Species	Gas	Surface	Gas	Surface	Gas	Surface	Surface
C4H2	1.1E-11	8.7E-12	9.6E-12	4.3E-11	1.0E-10	2.0E-09	2.8E-11
C5H	1.2E-13	5.9E-21	2.0E-13	1.9E-20	5.3E-12	4.0E-18	0.0E+00
C6	6.5E-14	1.4E-20	3.1E-13	1.7E-19	7.4E-11	7.7E-17	0.0E+00
C5N	3.7E-13	4.0E-19	7.6E-13	4.8E-18	7.5E-12	7.7E-16	0.0E+00
*CH5N	1.5E-11	3.3E-12	1.7E-11	1.1E-11	1.7E-11	3.9E-11	5.9E-11
C2H5		1.1E-15		3.0E-15		1.9E-14	1.1E-16
C3H4	1.3E-12	1.0E-11	8.9E-13	3.2E-11	3.4E-12	2.5E-10	4.5E-09
C4H3		6.4E-18		3.1E-17		1.5E-15	2.0E-17
*C2H4O	1.4E-13	3.1E-14	9.0E-14	7.5E-14	1.7E-13	2.2E-13	5.3E-13
C3H3N	5.1E-14	2.0E-11	4.8E-14	8.4E-11	9.0E-14	1.2E-09	4.5E-08
C5H2	3.3E-13	4.3E-14	4.6E-13	1.3E-13	7.0E-12	3.1E-12	3.8E-14
C6H	1.9E-14	1.8E-20	4.0E-14	2.0E-19	1.5E-12	7.8E-17	0.0E+00
HC5N	2.7E-13	1.9E-13	3.7E-13	1.4E-12	1.3E-12	1.8E-10	1.9E-12
C7	8.6E-15	1.6E-22	5.0E-14	1.4E-21	1.7E-11	1.1E-18	0.0E+00
*CH3C3N	1.7E-14	3.0E-15	1.9E-14	8.5E-15	4.8E-14	4.8E-14	7.3E-14
C5H2N		1.4E-19		1.0E-18		1.3E-16	1.4E-18
C2H6		6.9E-10		2.2E-09		1.2E-08	1.4E-07
C4H4		3.8E-12		1.6E-11		4.3E-10	2.4E-08
C5H3		3.2E-20		9.4E-20		2.3E-18	2.8E-20
C6H2	2.1E-13	2.8E-14	3.1E-13	1.2E-13	1.5E-11	1.8E-11	2.7E-13
C7H	2.2E-15	5.7E-23	6.3E-15	2.4E-22	3.2E-13	9.3E-20	0.0E+00
C8	9.9E-16	1.9E-22	7.5E-15	3.7E-21	4.7E-12	4.2E-18	0.0E+00
C7N	3.9E-15	2.3E-21	1.2E-14	3.1E-20	3.2E-13	1.6E-17	0.0E+00
*CH3OCH3	8.1E-17	1.3E-17	1.0E-16	4.9E-17	1.4E-16	2.1E-16	3.4E-16
*C2H5OH	6.8E-15	1.5E-15	3.2E-15	3.2E-15	6.8E-15	8.1E-15	1.8E-14
*CH3C4H	2.3E-13	3.7E-14	2.9E-13	1.1E-13	3.3E-12	1.6E-12	6.3E-12
C5H4		2.7E-14		7.3E-14		7.8E-13	3.4E-11
C6H3		2.1E-20		8.8E-20		1.3E-17	2.0E-19
C7H2	2.6E-15	2.8E-16	7.2E-15	1.2E-15	3.9E-13	1.1E-13	1.2E-15
C8H	4.4E-16	2.7E-22	1.6E-15	4.5E-21	1.8E-13	4.4E-18	0.0E+00
HC7N	3.7E-15	1.3E-15	9.3E-15	9.7E-15	2.1E-13	3.2E-12	5.0E-14
C9	7.4E-17	1.2E-24	6.5E-16	1.6E-23	6.1E-13	3.5E-20	0.0E+00
C5H3N		7.3E-14		4.1E-13		3.2E-11	1.9E-09
*CH3C5N	1.7E-17	2.2E-18	2.6E-17	7.8E-18	1.4E-16	8.6E-17	1.4E-16
C7H2N		9.9E-22		7.2E-21		2.3E-18	3.7E-20
C6H4		1.3E-14		4.9E-14		2.8E-12	2.7E-10
C7H3		2.0E-22		9.0E-22		7.8E-20	9.0E-22
C8H2	4.6E-16	1.4E-16	6.1E-16	1.1E-15	8.8E-14	7.4E-13	2.1E-14
C9H	6.4E-18	2.2E-25	1.9E-17	1.3E-24	3.2E-15	2.5E-21	0.0E+00
C9N	9.5E-18	1.3E-23	2.7E-17	2.9E-22	1.6E-15	4.9E-19	0.0E+00
*CH3C6H	1.4E-16	2.0E-17	1.8E-16	6.1E-17	8.0E-15	2.1E-15	1.3E-14
C7H4		1.7E-16		5.2E-16		2.0E-14	1.2E-12
C8H3		1.0E-22		7.9E-22		5.5E-19	1.6E-20
C9H2	1.0E-17	1.1E-18	2.7E-17	4.1E-18	4.3E-15	1.1E-15	2.5E-17
HC9N	8.9E-18	6.0E-18	2.0E-17	6.5E-17	1.1E-15	8.3E-14	1.6E-15
C7H3N		5.2E-16		2.8E-15		4.5E-13	5.0E-11

t(yr)	1.0E+05		3.2E+05		1.0E+06		1.0E+07
Species	Gas	Surface	Gas	Surface	Gas	Surface	Surface
*CH3C7N	2.1E-19	2.3E-20	6.1E-19	1.1E-19	2.0E-17	6.3E-18	1.7E-17
C9H2N		4.4E-24		4.8E-23		6.2E-20	1.2E-21
C8H4		5.8E-17		3.0E-16		9.4E-14	2.0E-11
C9H3		7.8E-25		3.0E-24		8.0E-22	1.8E-23
C9H4		7.1E-19		1.9E-18		1.5E-16	2.3E-14
C9H3N		2.1E-18		1.5E-17		1.0E-14	1.6E-12
E	3.6E-08		3.6E-08		4.7E-08		
H+	3.4E-10		5.0E-10		1.2E-09		
HE+	4.1E-10		6.5E-10		2.4E-09		
C+	2.0E-09		2.9E-09		6.3E-09		
N+	1.4E-11		1.6E-11		1.6E-11		
O+	4.1E-14		3.9E-14		2.8E-14		
NA+	2.7E-09		2.4E-09		1.6E-09		
MG+	9.2E-09		8.0E-09		5.2E-09		
SI+	1.7E-11		1.6E-11		6.9E-12		
S+	3.7E-10		3.0E-10		8.6E-11		
FE+	4.6E-09		4.4E-09		4.2E-09		
O2+	5.3E-10		4.8E-10		1.7E-10		
CH+	7.4E-17		1.9E-16		2.5E-15		
SO+	4.1E-11		2.9E-11		6.9E-12		
H3+	2.4E-09		4.0E-09		1.6E-08		
HCO+	1.1E-08		1.1E-08		6.9E-09		
HOC+	3.9E-10		4.7E-10		4.6E-10		
N2H+	2.4E-10		2.8E-10		1.9E-10		
HCS+	8.4E-11		8.7E-11		2.6E-11		
OCS+	2.3E-10		1.3E-10		6.5E-12		
H3O+	1.1E-09		1.0E-09		1.2E-09		
HCO2+	1.6E-12		1.8E-12		7.6E-13		
H2CN+	2.4E-11		4.4E-11		9.4E-11		
NH4+	1.4E-10		1.6E-10		1.7E-10		
CH5+	9.8E-12		1.8E-11		8.7E-11		
C4H2+	3.7E-13		9.2E-13		1.7E-11		
GRAIN0	1.4E-14		1.6E-14		2.4E-14		
GRAIN-	2.6E-12		2.6E-12		2.6E-12		

NOTES.—An asterisk indicates that a surface species is formed by accretion only. Numbers less than 1×10^{-39} have been truncated and are presented as 0.0. For some molecules, results are given for all isomers and for one particular isomer, e.g., C_5H_4 and CH_3C_4H.

TABLE 6

GAS AND SURFACE ABUNDANCES FOR MODEL B EXPRESSED AS A FRACTION OF TOTAL H_2 + 0.5H

t(yr)	1.0E+05		3.2E+05		1.0E+06		1.0E+07
Species	Gas	Surface	Gas	Surface	Gas	Surface	Surface
H	6.0E-01	2.6E-17	4.4E-02	3.4E-19	1.2E-04	1.2E-23	8.9E-24
*HE	2.8E-01	1.5E-21	2.8E-01	1.5E-21	2.8E-01	1.5E-21	1.5E-21
C	6.1E-05	1.3E-17	4.4E-06	6.8E-17	5.2E-08	2.7E-22	1.9E-28
N	3.1E-05	6.3E-18	1.5E-05	2.4E-16	1.5E-06	4.4E-14	3.8E-25
O	2.2E-04	4.2E-17	8.3E-05	8.7E-16	5.6E-06	1.6E-20	1.2E-24
NA	3.9E-10	6.1E-23	8.2E-10	9.9E-21	5.4E-10	1.8E-16	8.0E-18
MG	1.7E-09	2.6E-22	3.1E-09	3.7E-20	2.0E-09	6.7E-16	2.5E-17
SI	1.2E-08	1.8E-21	8.1E-09	9.0E-20	1.5E-09	4.7E-16	5.7E-22
S	1.2E-07	1.7E-20	7.3E-08	7.5E-19	2.0E-08	5.9E-15	3.3E-19
FE	1.6E-10	1.6E-23	6.1E-10	4.8E-21	4.2E-10	9.2E-17	7.6E-18
H2	7.0E-01	4.6E-06	9.8E-01	4.1E-06	1.0E+00	4.0E-06	4.0E-06
CH	1.3E-08	1.0E-17	1.4E-09	6.2E-20	1.0E-09	1.1E-24	3.1E-33
NH	5.3E-11	6.3E-18	1.4E-10	2.4E-16	1.2E-10	4.4E-17	3.8E-25
OH	1.1E-08	4.2E-17	3.4E-08	8.5E-16	1.3E-07	4.5E-16	2.1E-21
C2	5.2E-08	8.0E-21	1.4E-08	1.7E-19	1.4E-08	1.1E-15	1.9E-34
NAH	2.5E-14	9.3E-11	1.2E-13	4.7E-10	5.1E-14	1.6E-09	3.5E-09
MGH	7.9E-15	2.6E-22	1.5E-13	3.7E-20	2.4E-14	6.7E-16	2.5E-17
FEH		3.0E-11		1.8E-10		7.7E-10	1.8E-09
CN	4.3E-08	6.5E-21	2.7E-08	3.2E-19	3.6E-09	1.2E-15	4.6E-24
N2	4.6E-09	8.5E-16	6.1E-08	8.7E-13	1.1E-07	3.6E-07	1.7E-22
CO	4.3E-05	2.4E-12	5.4E-05	1.3E-10	1.2E-05	9.9E-07	2.2E-18
SIH	1.0E-10	1.8E-21	1.1E-10	9.1E-20	2.9E-10	5.6E-16	6.1E-22
NO	1.6E-09	3.1E-18	1.8E-08	6.8E-17	3.2E-08	1.0E-14	2.5E-24
O2	3.4E-07	6.0E-14	3.2E-06	3.4E-11	4.0E-06	1.2E-06	5.5E-21
HS	8.2E-11	1.5E-13	9.2E-11	4.5E-13	2.8E-11	8.6E-13	1.0E-12
*SIC	1.1E-10	2.5E-11	1.7E-11	4.4E-11	5.3E-12	5.4E-11	5.7E-11
*SIO	1.7E-10	1.4E-11	2.6E-10	1.1E-10	2.4E-11	2.5E-10	2.6E-10
CS	1.1E-09	4.6E-17	2.0E-09	3.6E-15	4.8E-10	3.2E-11	7.9E-22
*NS	1.5E-11	7.8E-13	7.5E-11	2.2E-11	2.6E-12	4.9E-11	5.0E-11
SO	1.4E-10	1.1E-14	7.1E-10	2.8E-15	1.2E-10	2.4E-11	4.1E-19
*SIS	1.5E-12	6.7E-14	5.3E-12	1.7E-12	7.4E-14	3.1E-12	3.2E-12
CH2	1.8E-07	1.3E-17	8.8E-08	6.9E-17	4.7E-09	2.5E-15	1.3E-23
NH2	6.3E-10	6.3E-18	2.3E-09	2.4E-16	4.0E-09	3.5E-16	3.8E-25
H2O	5.9E-08	8.4E-05	3.1E-07	1.7E-04	1.8E-07	2.2E-04	2.3E-04
SIH2		1.8E-21		9.1E-20		5.6E-16	6.1E-22
MGH2		4.0E-10		1.9E-09		6.1E-09	1.3E-08
C2H	3.3E-08	1.3E-20	9.9E-09	2.9E-19	2.8E-09	2.0E-15	2.0E-34
N2H		1.1E-14		4.5E-13		8.9E-11	1.3E-10
O2H		4.6E-20		2.7E-17		9.0E-13	4.3E-27
HCN	7.8E-09	8.6E-09	7.9E-09	3.6E-08	1.1E-09	5.3E-08	5.8E-08

t(yr)	1.0E+05		3.2E+05		1.0E+06		1.0E+07
Species	Gas	Surface	Gas	Surface	Gas	Surface	Surface
HNC	6.9E-10	3.9E-11	3.8E-09	2.1E-09	1.0E-09	4.9E-09	6.1E-09
HCO	7.9E-13	7.2E-14	4.3E-12	3.9E-13	3.9E-10	2.0E-12	8.0E-13
HOC		3.1E-18		1.7E-16		1.3E-12	2.9E-24
HCS		3.7E-10		8.4E-10		1.6E-09	1.8E-09
HNO	1.1E-12	1.1E-10	1.9E-12	5.5E-09	1.5E-13	7.7E-08	1.0E-07
H2S	5.3E-12	2.2E-08	8.6E-11	6.6E-08	7.5E-11	1.3E-07	1.5E-07
C3	3.8E-08	4.9E-21	1.0E-08	1.0E-19	1.4E-08	9.2E-16	3.4E-40
O3		4.4E-19		4.0E-13		6.9E-09	3.4E-27
C2N	2.2E-09	2.7E-22	5.1E-09	4.8E-20	6.3E-11	3.5E-15	9.6E-38
*NAOH	4.5E-17	1.4E-18	3.1E-15	6.4E-16	7.3E-16	3.0E-15	3.8E-15
OCN	3.0E-11	7.1E-15	7.2E-10	3.4E-14	1.5E-10	2.6E-10	2.3E-10
CO2	8.3E-11	8.1E-10	5.6E-09	2.8E-06	2.8E-09	2.6E-05	2.9E-05
OCS	2.4E-09	1.0E-10	1.2E-08	3.3E-09	5.2E-10	8.7E-09	8.9E-09
SO2	3.2E-12	7.0E-12	3.8E-11	2.0E-10	2.6E-12	6.9E-10	7.7E-10
CH3	4.3E-09	1.3E-17	7.2E-09	6.9E-17	2.9E-08	1.5E-14	3.1E-23
NH3	6.4E-10	1.2E-05	3.0E-09	2.7E-05	4.9E-09	3.5E-05	3.5E-05
SIH3		1.8E-21		9.1E-20		5.6E-16	6.1E-22
C2H2	1.5E-07	4.7E-14	1.4E-07	2.6E-12	3.4E-08	1.1E-08	8.4E-22
N2H2		3.5E-10		1.4E-08		2.8E-06	4.0E-06
H2O2		1.8E-13		1.1E-10		1.7E-06	4.2E-11
H2CO	1.1E-08	2.8E-06	4.2E-08	1.5E-05	7.2E-09	2.6E-05	3.1E-05
CHOH		3.1E-18		1.7E-16		1.3E-12	2.9E-24
HCCN		2.7E-22		4.8E-20		3.5E-15	9.6E-38
C3H	8.2E-09	5.9E-21	6.1E-09	1.6E-19	1.1E-09	2.9E-16	3.6E-40
*H2CS	5.4E-11	3.0E-12	2.5E-10	7.4E-11	9.5E-12	1.5E-10	1.6E-10
C4	3.6E-08	3.9E-21	7.7E-09	6.5E-20	9.5E-09	2.3E-15	0.0E+00
C3N	6.2E-09	6.6E-22	6.1E-09	5.1E-20	2.6E-10	3.0E-15	2.5E-37
C3O	1.2E-11	7.6E-13	3.7E-11	1.1E-11	3.1E-12	2.9E-11	3.0E-11
CH4	1.5E-07	3.4E-05	8.6E-07	5.2E-05	1.3E-07	5.4E-05	5.5E-05
SIH4		2.1E-09		7.3E-09		1.4E-08	1.6E-08
C2H3	9.7E-09	3.6E-20	1.4E-08	2.1E-18	3.8E-09	9.7E-15	6.2E-28
*CH3N	2.0E-12	8.7E-14	2.6E-11	1.0E-11	5.8E-12	2.2E-11	2.9E-11
C3H2	1.0E-08	9.7E-15	8.0E-09	3.2E-13	1.5E-09	6.6E-10	9.9E-23
C2H2N	1.7E-10	2.9E-22	7.1E-10	5.5E-20	1.1E-11	3.5E-15	9.6E-38
*C2H2O	1.2E-09	5.1E-11	2.5E-09	1.4E-09	4.7E-11	2.0E-09	2.0E-09
*CH2O2	1.1E-11	2.7E-13	8.1E-10	1.4E-10	7.0E-11	5.7E-10	6.1E-10
CH2OH		3.1E-18		1.7E-16		1.3E-12	2.9E-24
C4H	3.0E-08	7.2E-21	1.3E-08	1.7E-19	1.6E-09	2.6E-15	0.0E+00
HC3N	1.2E-09	1.1E-15	5.1E-09	1.2E-13	1.6E-10	3.0E-09	6.9E-23
C5	1.3E-08	1.3E-21	2.1E-09	1.6E-20	1.6E-09	7.7E-17	0.0E+00
*C4N	4.6E-10	2.6E-11	3.6E-10	2.2E-10	6.7E-12	2.9E-10	3.0E-10
C2H4	3.7E-11	2.5E-15	4.6E-10	1.4E-13	1.9E-11	6.3E-10	4.4E-23
CH3OH	8.5E-12	2.8E-06	1.3E-10	1.5E-05	9.8E-12	2.6E-05	3.1E-05
C3H3	3.3E-12	7.2E-21	3.4E-11	2.4E-19	1.7E-12	4.8E-16	7.3E-29
C2H3N	1.4E-11	1.2E-10	4.0E-11	3.0E-09	7.3E-13	1.1E-08	3.0E-08
C3H2N		8.0E-22		9.2E-20		2.2E-15	5.1E-29

TABLE 6—*Continued*

t(yr)	1.0E+05		3.2E+05		1.0E+06		1.0E+07
Species	Gas	Surface	Gas	Surface	Gas	Surface	Surface
C4H2	7.6E-10	9.8E-15	2.5E-09	2.6E-13	1.6E-10	2.0E-09	6.3E-23
C5H	2.9E-10	1.3E-21	1.5E-10	1.7E-20	9.5E-12	1.9E-17	0.0E+00
C6	1.8E-09	1.6E-22	4.1E-10	2.8E-21	1.8E-10	3.4E-17	0.0E+00
C5N	5.0E-10	4.4E-23	3.4E-10	2.3E-21	5.3E-12	2.5E-16	0.0E+00
*CH5N	1.3E-12	5.3E-14	1.8E-11	6.7E-12	3.8E-12	1.5E-11	1.9E-11
C2H5		3.6E-20		2.1E-18		9.4E-15	6.5E-28
C3H4	6.4E-12	8.0E-09	9.8E-11	2.7E-08	4.1E-12	3.8E-08	5.0E-08
C4H3		7.3E-21		1.9E-19		1.5E-15	4.6E-29
*C2H4O	6.7E-14	1.8E-15	1.5E-12	4.0E-13	1.8E-13	1.1E-12	1.3E-12
C3H3N	2.2E-13	3.9E-10	1.1E-11	5.7E-09	3.7E-14	1.2E-08	5.0E-08
C5H2	5.1E-11	1.8E-15	2.8E-10	2.6E-14	1.0E-11	2.1E-11	6.1E-25
C6H	5.8E-11	1.7E-22	6.4E-11	3.3E-21	2.7E-12	3.5E-17	0.0E+00
HC5N	4.3E-11	6.5E-17	1.3E-10	4.3E-15	7.5E-13	2.3E-10	1.4E-24
C7	3.8E-10	3.2E-23	1.5E-10	9.6E-22	4.3E-11	1.8E-18	0.0E+00
*CH3C3N	4.6E-13	9.7E-15	6.8E-12	2.4E-12	2.7E-14	3.2E-12	3.2E-12
C5H2N		4.8E-23		3.2E-21		1.7E-16	1.1E-30
C2H6		3.2E-08		1.6E-07		2.8E-07	4.0E-07
C4H4		7.3E-09		2.6E-08		3.6E-08	6.4E-08
C5H3		1.3E-21		1.9E-20		1.5E-17	4.5E-31
C6H2	2.8E-10	2.6E-16	6.6E-10	1.0E-14	3.2E-11	3.1E-11	2.6E-25
C7H	1.5E-11	3.3E-23	2.0E-11	1.1E-21	5.7E-13	4.5E-19	0.0E+00
C8	1.3E-10	9.8E-24	5.1E-11	3.0E-22	1.4E-11	2.4E-18	0.0E+00
C7N	1.8E-11	1.4E-24	3.0E-11	1.8E-22	2.1E-13	6.0E-18	0.0E+00
*CH3OCH3	2.9E-16	6.7E-18	1.6E-14	4.8E-15	1.4E-16	6.9E-15	7.1E-15
*C2H5OH	1.2E-15	2.3E-17	3.0E-13	5.7E-14	7.5E-15	1.5E-13	1.5E-13
*CH3C4H	2.1E-11	5.3E-13	2.2E-10	6.6E-11	4.9E-12	1.1E-10	1.1E-10
C5H4		1.6E-09		4.0E-09		4.8E-09	5.1E-09
C6H3		1.9E-22		7.7E-21		2.3E-17	1.9E-31
C7H2	1.7E-11	4.7E-17	2.7E-11	1.7E-15	7.1E-13	5.8E-13	1.2E-26
C8H	2.0E-11	1.1E-23	1.6E-11	4.0E-22	4.5E-13	2.5E-18	0.0E+00
HC7N	2.5E-12	2.1E-18	2.1E-11	4.1E-16	1.3E-13	5.4E-12	3.5E-26
C9	2.8E-11	2.1E-24	1.1E-11	6.2E-23	2.1E-12	7.9E-20	0.0E+00
C5H3N		2.8E-11		2.6E-10		6.3E-10	2.8E-09
*CH3C5N	1.1E-14	2.2E-16	1.1E-13	4.1E-14	8.3E-17	4.9E-14	4.9E-14
C7H2N		1.6E-24		3.0E-22		4.0E-18	2.6E-32
C6H4		1.6E-10		8.1E-10		1.1E-09	1.4E-09
C7H3		3.4E-23		1.3E-21		4.3E-19	8.7E-33
C8H2	3.5E-12	1.6E-17	1.8E-11	6.9E-16	2.3E-13	1.8E-12	2.8E-26
C9H	3.1E-13	2.1E-24	7.4E-13	6.7E-23	7.0E-15	1.9E-20	0.0E+00
C9N	9.1E-13	6.3E-26	1.0E-12	5.4E-24	1.9E-15	2.6E-19	0.0E+00
*CH3C6H	6.4E-14	1.0E-15	1.5E-12	3.7E-13	1.3E-14	5.6E-13	5.7E-13
C7H4		2.1E-11		1.5E-10		1.8E-10	1.9E-10
C8H3		1.2E-23		5.1E-22		1.3E-18	2.1E-32
C9H2	1.9E-13	2.9E-18	1.3E-12	1.0E-16	9.1E-15	2.0E-14	3.1E-28
HC9N	8.6E-14	9.3E-20	6.6E-13	1.2E-17	1.2E-15	2.2E-13	1.2E-27
C7H3N		5.0E-13		2.1E-11		3.5E-11	9.2E-11

t(yr)	1.0E+05		3.2E+05		1.0E+06		1.0E+07
Species	Gas	Surface	Gas	Surface	Gas	Surface	Surface
*CH3C7N	6.3E-16	8.0E-18	1.6E-14	5.5E-15	1.4E-17	6.5E-15	6.5E-15
C9H2N		6.9E-26		8.9E-24		1.6E-19	8.8E-34
C8H4		4.8E-12		5.8E-11		7.3E-11	1.0E-10
C9H3		2.1E-24		7.4E-23		1.5E-20	2.3E-34
C9H4		9.0E-13		9.5E-12		1.1E-11	1.2E-11
C9H3N		2.0E-14		7.6E-13		1.2E-12	3.6E-12
E	1.2E-07		4.5E-08		5.3E-08		
H+	3.5E-08		2.3E-09		1.5E-09		
HE+	1.2E-09		9.2E-10		2.8E-09		
C+	5.0E-08		9.9E-09		7.8E-09		
N+	7.0E-12		3.1E-12		4.3E-12		
O+	5.7E-15		1.1E-14		2.5E-14		
NA+	3.5E-09		2.7E-09		1.8E-09		
MG+	1.2E-08		9.0E-09		5.9E-09		
SI+	1.1E-09		5.6E-11		9.4E-12		
S+	9.1E-09		8.7E-10		1.0E-10		
FE+	5.8E-09		5.2E-09		4.8E-09		
O2+	9.8E-11		1.6E-10		1.2E-10		
CH+	1.5E-13		3.8E-14		2.8E-15		
SO+	2.7E-11		2.8E-11		6.7E-12		
H3+	1.5E-09		4.0E-09		2.0E-08		
HCO+	1.2E-09		6.7E-09		6.2E-09		
HOC+	1.2E-10		5.3E-10		4.3E-10		
N2H+	2.5E-14		2.2E-12		1.9E-11		
HCS+	6.6E-11		3.2E-11		2.3E-11		
OCS+	2.0E-10		1.2E-10		4.5E-12		
H3O+	4.4E-10		1.2E-09		1.1E-09		
HCO2+	1.0E-14		3.5E-13		4.8E-13		
H2CN+	1.0E-11		6.3E-11		3.3E-11		
NH4+	6.2E-12		1.6E-11		3.7E-11		
CH5+	1.5E-10		2.6E-10		1.0E-10		
C4H2+	4.8E-10		1.1E-10		2.7E-11		
GRAIN0	3.0E-14		1.8E-14		2.5E-14		
GRAIN-	2.6E-12		2.6E-12		2.6E-12		

NOTES.—An asterisk indicates that a surface species is formed by accretion only. Numbers less than 1×10^{-39} have been truncated and are presented as 0.0. For some molecules, results are given for all isomers and for one particular isomer, e.g., C_5H_4 and CH_3C_4H.

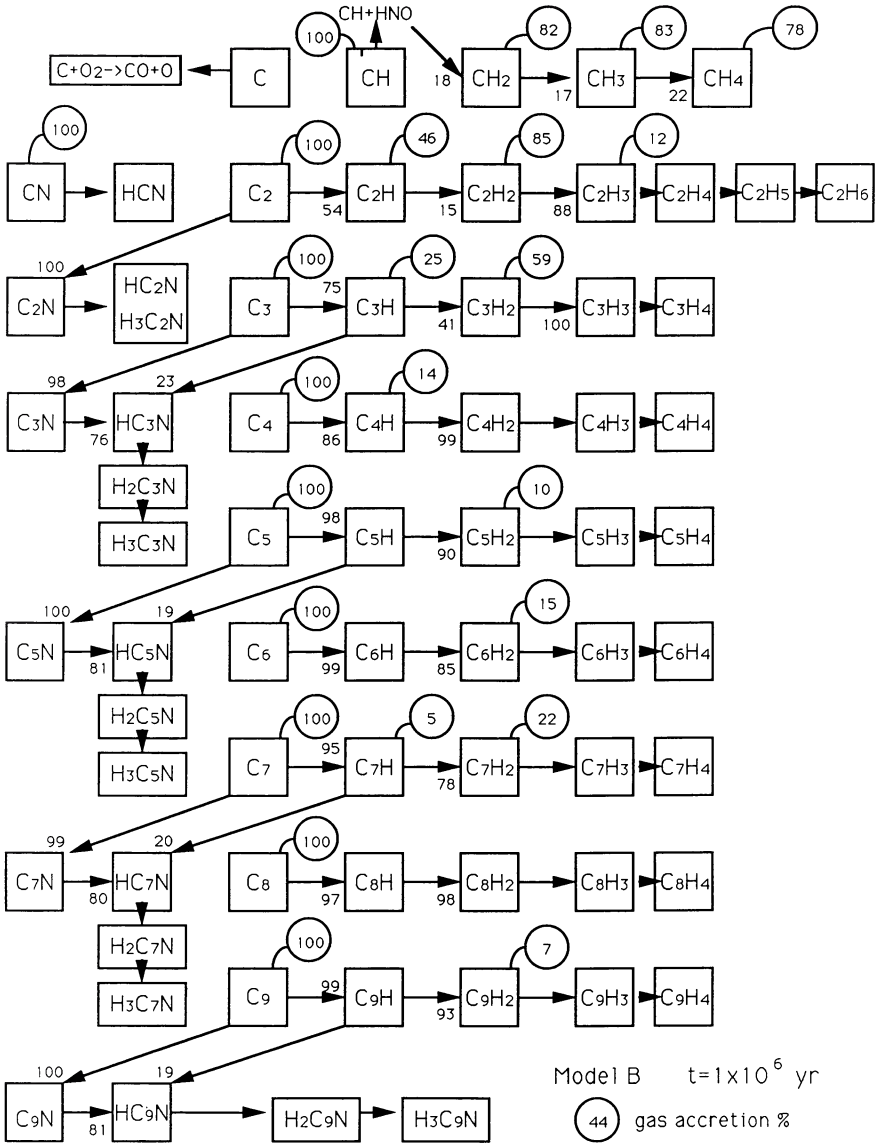

FIG. 8.—Formation pathways to hydrocarbons and organo-nitrogen species on grain surfaces at a time 1×10^6 yr for model B. The numbers at the arrow tips refer to the relative contributions (%) of assorted precursors to the syntheses of the species shown. Relative contributions from accretion of the gas-phase species are shown by encircled numbers.

so that by 10^7 yr all organo-nitrogen material is in the most saturated form available. Peak abundances of the cyanopolyynes on grain surfaces are comparable to those achieved in the gas at an earlier era.

3.3. *Model C*

The initial abundances utilized here are the standard set found in pseudo–time-dependent gas-phase models (see Table 4), in which the hydrogen is molecular and the easily ionized heavy atoms are found in their ionized form. Not surprisingly, therefore, the gas-phase chemistry through "early time" resembles that of the purely gas-phase models, with peak abundances of complex molecules occurring at approximately 1×10^5 yr, well before accretion depletes the gas phase significantly. Agreement with observed abundances in TMC-1 at this time is good (HL2). An atomic hydrogen abundance in the gas of ≈ 1 cm^{-3} is maintained. The abundances of the dominant surface species and their gaseous antecedents are shown in Figure 3 as a function of time. Table 7 contains a more complete listing of gaseous and surface abundances at selected times. As the asymptotic surface abundances are reached, model C bears more of a resemblance to the hydrogen-poor model A than to the hydrogen-rich model B *in these dominant species.* Specifically, as also shown in Table 4, although the atoms oxygen and sulfur are hydrogenated to their saturated forms (H_2O, H_2S), carbon and nitrogen are much less efficiently hydrogenated to methane and ammonia. The dominant forms of these elements on the grains are CO_2 and N_2H_2, respectively; methanol and formaldehyde are not as abundant as in model A. The

TABLE 7

GAS AND SURFACE ABUNDANCES FOR MODEL C EXPRESSED AS A FRACTION OF TOTAL H_2 + 0.5H

t(yr)	1.0E+05		3.2E+05		1.0E+06		1.0E+07
Species	Gas	Surface	Gas	Surface	Gas	Surface	Surface
H	2.0E-04	3.6E-23	1.2E-04	7.4E-24	1.0E-04	2.7E-24	2.2E-24
*HE	2.8E-01	1.5E-21	2.8E-01	1.5E-21	2.8E-01	1.5E-21	1.5E-21
C	3.7E-05	2.6E-14	1.8E-06	1.8E-19	5.8E-08	6.5E-23	3.4E-29
N	3.1E-05	1.6E-13	1.5E-05	1.5E-13	1.5E-06	4.7E-14	1.6E-24
O	1.9E-04	1.8E-13	7.6E-05	3.2E-18	5.9E-06	3.3E-21	1.5E-27
NA	9.5E-10	1.1E-16	8.7E-10	4.8E-16	5.0E-10	7.7E-16	3.0E-17
MG	3.9E-09	4.3E-16	3.3E-09	1.8E-15	1.8E-09	2.8E-15	9.2E-17
SI	1.2E-08	1.3E-15	7.5E-09	3.8E-15	1.4E-09	2.0E-15	2.1E-21
S	7.9E-08	1.3E-15	6.4E-08	3.0E-14	2.0E-08	2.6E-14	1.3E-18
FE	1.1E-09	7.8E-17	8.5E-10	3.0E-16	4.0E-10	4.0E-16	2.9E-17
H2	1.0E+00	4.0E-06	1.0E+00	4.0E-06	1.0E+00	4.0E-06	4.0E-06
CH	4.2E-09	4.7E-24	9.5E-10	1.5E-26	1.1E-09	1.7E-26	6.8E-35
NH	4.9E-10	5.8E-17	1.6E-10	2.7E-17	1.1E-10	9.8E-18	1.6E-24
OH	2.1E-08	7.7E-15	3.5E-08	3.5E-15	1.2E-07	3.7E-16	8.3E-18
C2	2.5E-08	6.8E-15	1.0E-08	3.0E-16	1.5E-08	1.4E-15	8.6E-34
NAH	2.3E-13	1.6E-10	1.3E-13	6.8E-10	4.7E-14	1.8E-09	3.6E-09
MGH	8.3E-13	4.3E-16	1.8E-13	1.8E-15	2.0E-14	2.8E-15	9.2E-17
FEH		1.1E-10		4.6E-10		1.1E-09	2.1E-09
CN	7.2E-08	4.8E-13	2.2E-08	1.2E-14	3.7E-09	5.4E-15	1.1E-23
N2	3.1E-08	9.4E-07	1.3E-07	3.7E-06	1.2E-07	4.4E-06	3.0E-10
CO	6.7E-05	2.7E-12	6.0E-05	8.3E-08	1.3E-05	5.4E-06	4.7E-17
SIH	2.8E-11	1.3E-15	1.2E-10	3.8E-15	2.6E-10	2.3E-15	2.3E-21
NO	6.4E-09	8.5E-13	2.7E-08	1.4E-14	2.9E-08	4.2E-14	1.1E-23
O2	1.2E-06	2.3E-12	5.0E-06	6.0E-08	3.8E-06	5.3E-06	6.2E-10
HS	3.6E-11	4.7E-14	7.1E-11	1.4E-13	2.8E-11	5.2E-13	6.4E-13
*SIC	2.8E-11	2.5E-11	9.5E-12	3.3E-11	5.2E-12	4.1E-11	4.5E-11
*SIO	5.2E-10	1.5E-10	2.7E-10	3.0E-10	2.3E-11	4.3E-10	4.4E-10
CS	6.4E-09	3.4E-16	3.0E-09	3.2E-12	4.9E-10	1.8E-10	1.8E-20
*NS	2.1E-10	3.1E-11	9.1E-11	9.0E-11	2.5E-12	1.2E-10	1.2E-10
SO	1.6E-09	1.3E-15	1.0E-09	1.1E-12	1.1E-10	1.1E-10	7.6E-11
*SIS	1.2E-11	2.1E-12	6.3E-12	5.4E-12	7.2E-14	6.9E-12	6.9E-12
CH2	3.0E-07	1.2E-14	4.7E-08	3.4E-14	5.1E-09	1.2E-14	5.5E-23
NH2	7.6E-09	1.7E-16	2.6E-09	8.1E-17	3.8E-09	3.6E-16	1.6E-24
H2O	1.0E-06	2.9E-05	3.5E-07	6.2E-05	1.7E-07	8.6E-05	1.1E-04
SIH2		1.3E-15		3.8E-15		2.3E-15	2.3E-21
MGH2		6.5E-10		2.7E-09		6.8E-09	1.3E-08
C2H	6.2E-08	8.0E-15	8.4E-09	4.8E-15	3.0E-09	5.8E-15	9.4E-34
N2H		5.4E-11		1.6E-10		3.6E-10	5.2E-10
O2H		3.2E-14		4.6E-14		4.1E-12	4.8E-16
HCN	8.3E-08	1.9E-06	5.5E-09	2.7E-06	1.1E-09	2.7E-06	2.7E-06

t(yr)	1.0E+05		3.2E+05		1.0E+06		1.0E+07
Species	Gas	Surface	Gas	Surface	Gas	Surface	Surface
HNC	4.1E-08	2.7E-07	3.2E-09	2.9E-07	1.0E-09	2.9E-07	2.9E-07
HCO	2.2E-09	2.4E-15	6.8E-10	1.3E-13	4.5E-10	7.4E-12	3.9E-13
HOC		2.7E-15		1.1E-13		7.2E-12	6.2E-23
HCS		1.0E-14		3.6E-13		4.9E-10	8.3E-10
HNO	2.4E-11	3.0E-06	2.4E-12	5.0E-06	1.5E-13	5.0E-06	5.1E-06
H2S	5.3E-11	6.8E-09	9.4E-11	1.6E-08	7.1E-11	7.4E-08	9.5E-08
C3	2.0E-08	6.6E-16	7.9E-09	1.9E-16	1.6E-08	1.2E-15	1.7E-39
O3		5.3E-08		1.2E-07		3.0E-08	1.9E-18
C2N	2.5E-08	2.1E-13	5.7E-09	7.8E-15	7.3E-11	2.1E-14	1.6E-37
*NAOH	4.1E-14	6.3E-15	4.7E-15	1.2E-14	6.5E-16	1.5E-14	1.5E-14
OCN	1.7E-09	3.8E-12	1.3E-09	1.4E-11	1.5E-10	6.9E-10	7.3E-10
CO2	2.6E-07	2.7E-05	1.9E-07	6.8E-05	4.5E-09	9.8E-05	1.0E-04
OCS	4.3E-08	9.1E-09	1.7E-08	2.3E-08	5.4E-10	2.9E-08	2.9E-08
SO2	4.0E-10	1.2E-08	7.8E-11	3.4E-08	2.2E-12	3.5E-08	3.5E-08
CH3	4.9E-09	2.2E-15	5.5E-09	3.8E-14	2.9E-08	6.9E-14	1.3E-22
NH3	1.4E-08	9.4E-09	3.5E-09	1.5E-08	4.5E-09	2.2E-08	3.8E-08
SIH3		1.3E-15		3.8E-15		2.3E-15	2.3E-21
C2H2	2.6E-07	6.8E-08	1.5E-07	7.8E-08	3.7E-08	8.5E-08	2.9E-11
N2H2		1.7E-06		5.0E-06		1.1E-05	1.6E-05
H2O2		7.4E-08		8.3E-08		3.0E-06	7.0E-07
H2CO	1.7E-07	4.8E-07	3.9E-08	6.0E-07	7.7E-09	7.7E-06	1.5E-05
CHOH		2.7E-15		1.1E-13		7.2E-12	6.2E-23
HCCN		2.1E-13		7.8E-15		2.1E-14	1.6E-37
C3H	3.9E-08	1.7E-15	5.6E-09	1.4E-16	1.3E-09	1.6E-16	1.8E-39
*H2CS	1.0E-09	1.0E-10	3.8E-10	3.6E-10	9.8E-12	4.5E-10	4.6E-10
C4	1.7E-08	1.1E-15	5.4E-09	2.1E-15	1.1E-08	1.2E-14	0.0E+00
C3N	2.2E-08	1.5E-13	5.4E-09	5.3E-15	2.8E-10	1.9E-14	1.3E-36
C3O	3.1E-11	6.4E-08	5.3E-11	6.7E-08	3.7E-12	6.7E-08	6.7E-08
CH4	1.8E-06	8.1E-07	1.3E-06	2.1E-06	1.4E-07	2.9E-06	4.0E-06
SIH4		2.9E-09		7.7E-09		1.4E-08	1.6E-08
C2H3	5.4E-08	3.4E-14	1.4E-08	6.5E-14	4.1E-09	6.9E-14	2.1E-17
*CH3N	8.7E-10	1.5E-10	2.6E-11	2.9E-10	5.7E-12	3.0E-10	3.1E-10
C3H2	2.4E-08	9.4E-09	7.3E-09	5.6E-09	1.7E-09	3.9E-09	1.4E-12
C2H2N	2.8E-08	2.2E-13	9.7E-10	8.2E-15	1.2E-11	2.1E-14	1.6E-37
*C2H2O	3.6E-08	5.7E-09	2.9E-09	1.1E-08	5.4E-11	1.2E-08	1.2E-08
*CH2O2	1.0E-09	8.5E-11	1.1E-09	5.2E-10	7.4E-11	1.0E-09	1.1E-09
CH2OH		1.2E-14		1.1E-13		7.2E-12	6.2E-23
C4H	1.2E-07	1.2E-14	1.0E-08	6.0E-15	1.9E-09	1.4E-14	0.0E+00
HC3N	5.8E-08	2.1E-07	5.5E-09	1.1E-07	1.8E-10	4.5E-08	1.3E-11
C5	8.7E-09	2.4E-16	1.5E-09	2.8E-17	1.9E-09	1.1E-16	0.0E+00
*C4N	2.9E-09	3.1E-10	4.1E-10	7.6E-10	8.0E-12	8.4E-10	8.5E-10
C2H4	1.2E-09	2.3E-09	7.6E-10	4.3E-09	2.2E-11	4.6E-09	1.5E-12
CH3OH	3.2E-09	2.3E-07	1.2E-10	2.6E-07	1.0E-11	7.3E-06	1.4E-05
C3H3	1.8E-10	3.0E-14	6.8E-11	4.2E-15	2.0E-12	2.9E-15	1.1E-18
C2H3N	3.7E-09	8.1E-07	2.1E-11	1.1E-06	7.8E-13	1.1E-06	1.1E-06
C3H2N		1.5E-13		8.1E-14		3.3E-14	9.5E-18

TABLE 7—*Continued*

t(yr)	1.0E+05		3.2E+05		1.0E+06		1.0E+07
Species	Gas	Surface	Gas	Surface	Gas	Surface	Surface
C4H2	2.0E-08	1.8E-08	3.5E-09	1.4E-08	1.9E-10	1.2E-08	6.7E-12
C5H	4.2E-09	1.1E-16	1.8E-10	4.7E-18	1.2E-11	7.3E-18	0.0E+00
C6	3.4E-09	2.3E-16	3.6E-10	1.1E-16	2.3E-10	2.0E-16	0.0E+00
C5N	2.9E-09	1.1E-15	3.8E-10	6.2E-16	6.5E-12	1.7E-15	0.0E+00
*CH5N	6.4E-10	1.0E-10	1.9E-11	2.0E-10	3.8E-12	2.1E-10	2.2E-10
C2H5		3.4E-14		6.3E-14		6.9E-14	2.2E-17
C3H4	2.3E-10	2.8E-07	2.5E-10	3.2E-07	4.8E-12	3.2E-07	3.3E-07
C4H3		1.3E-14		1.0E-14		8.9E-15	4.9E-18
*C2H4O	1.4E-11	1.7E-12	2.5E-12	4.3E-12	1.9E-13	5.1E-12	5.3E-12
C3H3N	2.0E-10	4.0E-07	2.0E-11	6.6E-07	4.5E-14	7.5E-07	8.4E-07
C5H2	4.4E-09	6.1E-10	4.2E-10	4.6E-10	1.2E-11	1.8E-10	2.8E-14
C6H	2.0E-09	3.6E-16	6.9E-11	1.4E-16	3.5E-12	2.0E-16	0.0E+00
HC5N	5.1E-09	2.3E-09	1.9E-10	2.0E-09	9.4E-13	1.5E-09	5.6E-13
C7	1.5E-09	4.4E-17	1.3E-10	2.0E-18	5.7E-11	2.8E-18	0.0E+00
*CH3C3N	3.7E-10	4.7E-11	8.4E-12	7.8E-11	3.2E-14	7.9E-11	7.9E-11
C5H2N		1.7E-15		1.5E-15		1.1E-15	4.1E-19
C2H6		4.4E-07		5.3E-07		6.4E-07	8.5E-07
C4H4		6.9E-08		9.5E-08		1.1E-07	1.5E-07
C5H3		4.5E-16		3.4E-16		1.3E-16	2.0E-20
C6H2	4.5E-09	7.9E-10	6.9E-10	7.0E-10	4.0E-11	4.0E-10	9.8E-14
C7H	1.1E-09	2.2E-17	1.9E-11	3.9E-19	7.5E-13	2.0E-19	0.0E+00
C8	7.9E-10	4.4E-17	4.2E-11	1.1E-17	1.9E-11	1.5E-17	0.0E+00
C7N	5.4E-10	2.1E-16	2.6E-11	4.2E-17	2.7E-13	4.3E-17	0.0E+00
*CH3OCH3	3.0E-12	2.6E-13	1.8E-14	6.2E-13	1.5E-16	6.2E-13	6.2E-13
*C2H5OH	2.9E-12	2.2E-13	7.4E-13	9.5E-13	8.4E-15	1.1E-12	1.1E-12
*CH3C4H	3.3E-09	2.4E-10	3.8E-10	8.4E-10	6.1E-12	8.9E-10	9.0E-10
C5H4		4.8E-09		5.6E-09		6.0E-09	6.2E-09
C6H3		5.8E-16		5.2E-16		2.9E-16	7.2E-20
C7H2	9.3E-10	1.1E-10	2.8E-11	6.0E-11	9.4E-13	2.0E-11	2.2E-15
C8H	1.1E-09	1.1E-16	1.5E-11	1.5E-17	6.4E-13	1.5E-17	0.0E+00
HC7N	1.1E-09	4.0E-10	2.3E-11	2.8E-10	1.7E-13	1.2E-10	2.3E-14
C9	2.2E-10	8.4E-18	1.0E-11	1.4E-19	3.1E-12	1.3E-19	0.0E+00
C5H3N		5.3E-09		8.8E-09		1.1E-08	1.5E-08
*CH3C5N	2.6E-11	2.6E-12	1.2E-13	4.0E-12	1.1E-16	4.0E-12	4.0E-12
C7H2N		3.0E-16		2.0E-16		8.6E-17	1.7E-20
C6H4		2.9E-09		4.1E-09		4.7E-09	5.5E-09
C7H3		8.4E-17		4.4E-17		1.5E-17	1.6E-21
C8H2	5.5E-10	1.8E-10	4.1E-11	1.1E-10	3.1E-13	4.5E-11	1.0E-14
C9H	1.4E-10	3.1E-18	9.8E-13	2.1E-20	1.0E-14	8.4E-21	0.0E+00
C9N	6.9E-11	3.7E-17	1.5E-12	2.8E-18	2.7E-15	2.1E-18	0.0E+00
*CH3C6H	9.5E-11	6.2E-12	3.5E-12	1.6E-11	1.8E-14	1.7E-11	1.7E-11
C7H4		6.5E-10		7.9E-10		8.3E-10	8.5E-10
C8H3		1.3E-16		8.1E-17		3.3E-17	7.6E-21
C9H2	2.1E-10	2.0E-11	2.0E-12	9.7E-12	1.3E-14	3.0E-12	2.9E-16
HC9N	1.3E-10	7.2E-11	1.3E-12	3.8E-11	1.7E-15	1.3E-11	1.7E-15
C7H3N		7.6E-10		1.3E-09		1.6E-09	1.8E-09

t(yr)	1.0E+05		3.2E+05		1.0E+06		1.0E+07
Species	Gas	Surface	Gas	Surface	Gas	Surface	Surface
*CH3C7N	5.3E-12	4.8E-13	1.3E-14	7.3E-13	1.8E-17	7.3E-13	7.3E-13
C9H2N		5.3E-17		2.8E-17		9.8E-18	1.3E-21
C8H4		4.5E-10		6.8E-10		7.7E-10	8.5E-10
C9H3		1.5E-17		7.2E-18		2.2E-18	2.1E-22
C9H4		7.2E-11		9.7E-11		1.0E-10	1.1E-10
C9H3N		1.3E-10		2.2E-10		2.5E-10	2.7E-10
E	3.6E-08		4.1E-08		5.2E-08		
H+	3.0E-10		8.4E-10		1.5E-09		
HE+	6.4E-10		8.3E-10		2.7E-09		
C+	2.9E-09		8.0E-09		8.4E-09		
N+	5.6E-12		2.6E-12		4.2E-12		
O+	2.3E-15		1.4E-14		2.4E-14		
NA+	2.9E-09		2.4E-09		1.7E-09		
MG+	9.5E-09		8.0E-09		5.4E-09		
SI+	1.4E-11		3.6E-11		9.3E-12		
S+	2.0E-10		6.5E-10		1.1E-10		
FE+	4.8E-09		4.7E-09		4.5E-09		
O2+	9.1E-12		1.0E-10		1.2E-10		
CH+	1.8E-13		1.6E-14		3.0E-15		
SO+	1.3E-11		2.4E-11		6.9E-12		
H3+	2.2E-09		4.0E-09		1.9E-08		
HCO+	5.2E-09		8.1E-09		6.5E-09		
HOC+	4.9E-10		5.8E-10		4.5E-10		
N2H+	5.6E-13		4.9E-12		2.1E-11		
HCS+	2.0E-11		3.8E-11		2.3E-11		
OCS+	2.0E-10		1.4E-10		5.0E-12		
H3O+	2.0E-09		1.3E-09		1.1E-09		
HCO2+	4.5E-12		6.6E-12		7.3E-13		
H2CN+	4.1E-10		5.6E-11		3.3E-11		
NH4+	4.7E-11		1.6E-11		3.5E-11		
CH5+	4.0E-10		2.0E-10		1.1E-10		
C4H2+	4.0E-10		8.1E-11		3.2E-11		
GRAIN0	1.3E-14		1.6E-14		2.5E-14		
GRAIN-	2.6E-12		2.6E-12		2.6E-12		

NOTES.—An asterisk indicates that a species is formed by accretion only. Numbers less than 1×10^{-39} have been truncated and are presented as 0.0. For some molecules, results are given for all isomers and for one particular isomer, e.g., C_5H_4 and CH_3C_4H.

chemistry occurring on the grains is different from that in model A, since, among other reasons, the accreting gas here is not dominated by CO, at least initially.

The rather complex grain chemistry can be divided into an initial steady accretion phase, which lasts up to about 3×10^5 yr, an O_2/CO accretion phase, which occurs from 3×10^5 yr until 3×10^6 yr, and a hydrogenation phase, which lasts until the end of the calculation. The first phase is marked by accretion of heavy neutral atoms including C, which is formed rapidly in the gas from precursor C^+ (HL1). Hydrogenation to saturated forms competes with other processes. In the case of nitrogen, N atoms combine with H atoms to form NH, but also combine with each other to form N_2, and combine with NH to form N_2H (which leads to N_2H_2 formation). In the case of oxygen, O_2 and O_3 are formed preferentially, and the O_3 reacts with H to form OH + O_2, with the OH subsequently being hydrogenated to water (TH). Although the nitrogen and oxygen chemistries resemble those in model A, the case of carbon differs. Here the accreting carbon atoms combine mainly with O_2 to form CO and O. The CO is hydrogenated to formaldehyde and methanol and has a much lower abundance than in model A at this juncture.

The second (O_2/CO accretion) phase is characterized by accretion of a gas rich in these two species, enriching their surface abundances (Fig. 3). The enriched CO is partially hydrogenated, leading to increases in the abundances of surface formaldehyde and methanol (Fig. 3). During the third phase, most heavy atoms and molecules are substantially depleted from the gas. A significant gas-phase abundance of atomic hydrogen maintains an adsorption rate for this species, and slow hydrogenation reactions dominate the surface chemistry.

The hydrocarbon formation proceeds quite differently from that in model B. High surface abundances of saturated species are formed quite early (see Fig. 6); 20%–40% of the asymptotic abundances are produced before 3×10^4 yr. These species are synthesized mainly via grain-surface reactions from precursor C atoms by repeated C and H addition reactions on the surface. *This is efficient because the relatively low abundance of surface* H *does not immediately saturate all* C *into the unreactive* CH_4. Figure 9 shows a snapshot of the assorted hydrocarbon formation pathways for model C at 1×10^4 yr. At significantly later times, hydrocarbon formation on the grains is quite different and stems mainly from accretion of the unsaturated gas-phase species C_nH and C_nH_2. A snapshot of formation pathways at 1×10^5 yr is shown in Figure 10.

By the time asymptotic values of the surface hydrocarbon abundances are achieved, both accretion and grain-surface reactions have played important roles. For methane, as an example, three-fourths of the final surface abundance is due to direct accretion from the gas. On the other hand, 40% of C_2H_6 and 53% of C_3H_4 stem from surface reactions starting with accreting atomic carbon.

Figure 7 shows some of the surface organo-nitrogen abundances in model C as a function of time. Data on other species are contained in Table 7. By a time 1×10^5 yr, it can be seen that large abundances of cyanopolyynes ($HC_{2n}CN$) exist on the surface; these are as large as those found in the gas phase at the same time (Table 7). The more complex surface cyanopolyynes (HC_4CN etc.) are formed mainly by surface reactions from precursor carbon clusters via C and N addition; the formation routes are shown in Figure 10. The surface HC_3N stems mainly from surface CN. As time proceeds, the organonitrogen species are saturated to the full extent allowed in our model during the hydrogenation phase.

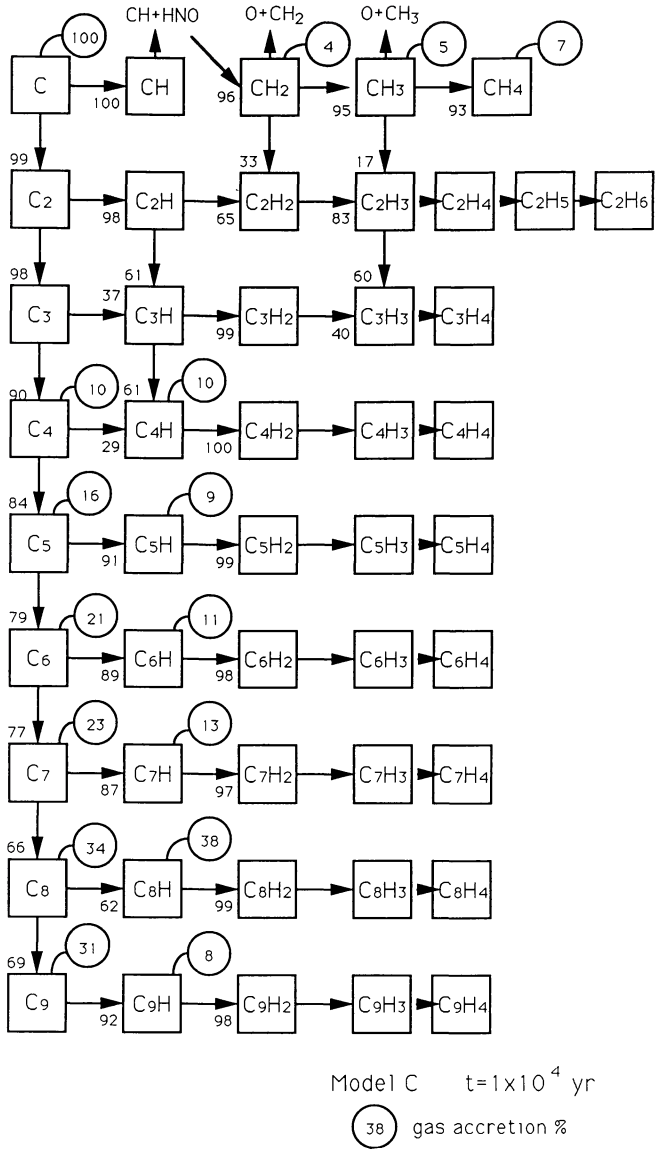

FIG. 9.—Formation pathways to hydrocarbons on grain surfaces at a time 1×10^4 yr for model C. Otherwise the same as Fig. 8.

3.4. *Model D*

This model differs from model C only in the omission of the surface reaction CO + O → CO_2 (Grim & d'Hendecourt 1986). The time dependences of the abundances of important species are depicted in Figure 4, while a more complete abundance listing is to be found in Table 8. The most salient difference between the results of models C and D is that the final CO_2 abundance in model D is lowered by a factor of ≈ 5 relative to its value in model C. Instead of constituting 37% of the final surface abundances, its abundance is reduced to 6% of the surface abundance, or a fractional abundance with respect to

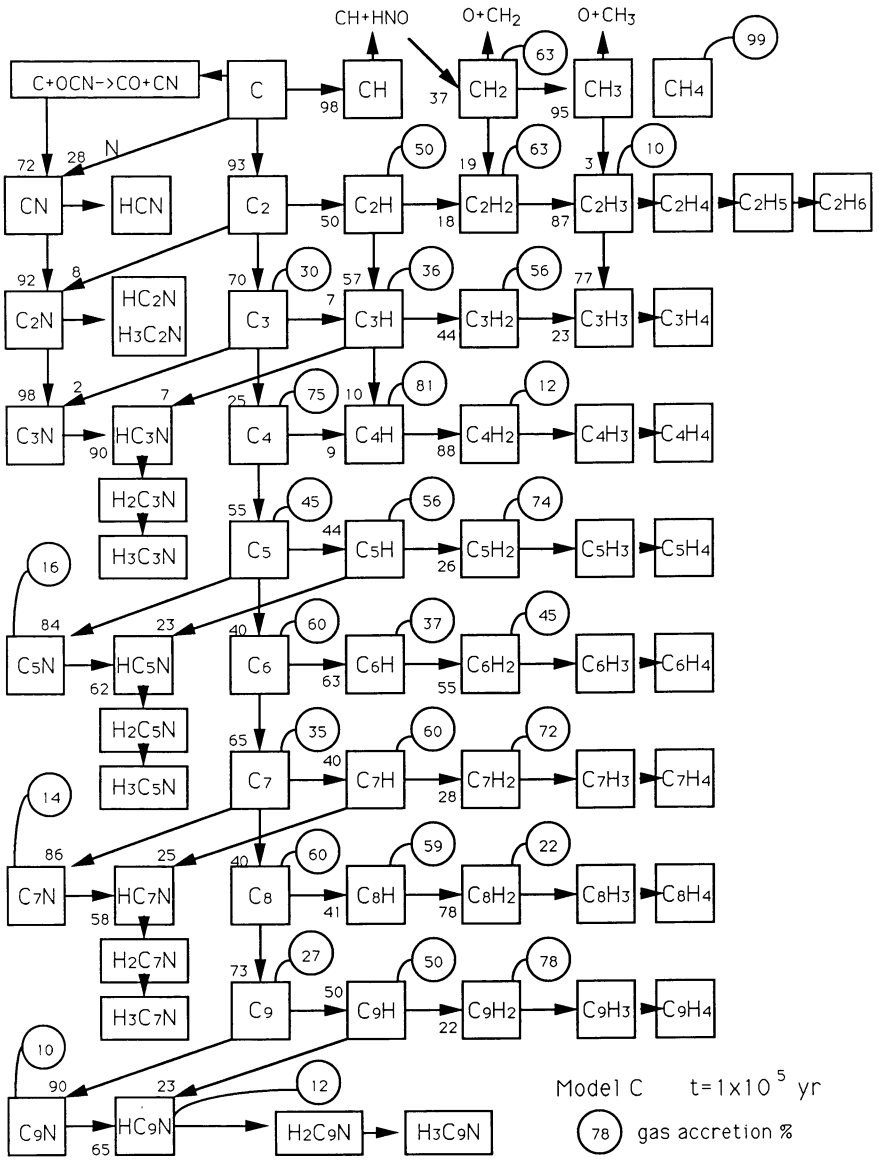

FIG. 10.—Formation pathways to hydrocarbons and organo-nitrogen species at a time 1×10^5 yr for model C. Otherwise the same as Fig. 8.

$n/2$ of 2×10^{-5} (Table 8). The reduced CO_2 surface abundance is largely compensated for by increases in the methanol and formaldehyde surface abundances. The alternative pathway which is here responsible for CO_2 formation is the reaction (Mitchell 1984) O + HCO → CO_2 + H. If this reaction truly occurs, CO_2 can be abundantly formed on grain surfaces without recourse to UV photolysis, which has been proposed as an alternative formation mechanism (Sandford & Allamandola 1990; Sandford et al. 1988; d'Hendecourt et al. 1985).

4. DISCUSSION

The calculations reported here are designed to extend our gas-phase models of dark clouds such as TMC-1 to include surface chemistry, in particular, the surface chemistry of organic molecules. Assuming that our grain-surface chemical processes bear some resemblance to reality, the gas-grain models will represent dark clouds accurately if nonthermal desorption mechanisms (e.g., photodesorption), which are excluded from the present work, do not greatly affect many of the results. The surface abundances here can be compared with those of previous models. They can also be compared, to a limited extent, with surface IR observations in dark clouds and other quiescent interstellar regions. The comparison with observations should also include the rich gas-phase data. Finally, we can compare our results with star formation regions such as the Orion hot core by making the assumption that the gas phase found in these regions results at least partially from a sudden evaporation of surface molecules due to heating. This comparison is similar to that undertaken by Brown et al. (1988), except that these authors used a much smaller grain-surface reaction network, and allowed the source to collapse

TABLE 8

GAS AND SURFACE ABUNDANCES FOR MODEL D EXPRESSED AS A FRACTION OF TOTAL H_2 + 0.5H

t(yr)	1.0E+05		3.2E+05		1.0E+06		1.0E+07
Species	Gas	Surface	Gas	Surface	Gas	Surface	Surface
H	2.0E-04	3.0E-23	1.2E-04	6.1E-24	1.0E-04	2.6E-24	2.2E-24
*HE	2.8E-01	1.5E-21	2.8E-01	1.5E-21	2.8E-01	1.5E-21	1.5E-21
C	3.7E-05	1.8E-14	1.8E-06	3.2E-18	5.8E-08	6.3E-23	3.4E-29
N	3.1E-05	1.6E-13	1.5E-05	1.5E-13	1.5E-06	4.7E-14	1.6E-24
O	1.9E-04	1.9E-13	7.6E-05	1.4E-16	5.9E-06	6.4E-21	1.5E-27
NA	9.5E-10	1.3E-16	8.7E-10	5.9E-16	5.0E-10	7.8E-16	3.0E-17
MG	3.9E-09	5.1E-16	3.3E-09	2.2E-15	1.8E-09	2.8E-15	9.2E-17
SI	1.2E-08	1.5E-15	7.5E-09	4.6E-15	1.4E-09	2.0E-15	2.1E-21
S	7.9E-08	1.3E-15	6.4E-08	3.6E-14	2.0E-08	2.7E-14	1.3E-18
FE	1.1E-09	9.2E-17	8.5E-10	3.7E-16	4.0E-10	4.0E-16	2.9E-17
H2	1.0E+00	4.0E-06	1.0E+00	4.0E-06	1.0E+00	4.0E-06	4.0E-06
CH	4.2E-09	2.4E-24	9.5E-10	1.4E-26	1.1E-09	1.5E-26	5.9E-35
NH	4.9E-10	4.9E-17	1.6E-10	2.2E-17	1.1E-10	9.6E-18	1.6E-24
OH	2.1E-08	1.3E-14	3.5E-08	8.2E-15	1.2E-07	7.0E-16	8.5E-18
C2	2.5E-08	3.6E-15	1.0E-08	3.0E-16	1.5E-08	1.4E-15	8.6E-34
NAH	2.3E-13	1.6E-10	1.3E-13	6.8E-10	4.7E-14	1.8E-09	3.6E-09
MGH	8.3E-13	5.1E-16	1.8E-13	2.2E-15	2.0E-14	2.8E-15	9.2E-17
FEH		1.1E-10		4.6E-10		1.1E-09	2.1E-09
CN	7.2E-08	5.3E-13	2.2E-08	1.4E-14	3.7E-09	5.5E-15	1.1E-23
N2	3.1E-08	1.1E-06	1.3E-07	4.0E-06	1.2E-07	4.8E-06	3.2E-10
CO	6.7E-05	4.4E-06	6.0E-05	1.2E-05	1.3E-05	1.0E-05	4.7E-17
SIH	2.8E-11	1.5E-15	1.2E-10	4.6E-15	2.6E-10	2.4E-15	2.3E-21
NO	6.4E-09	1.1E-12	2.7E-08	2.3E-14	2.9E-08	4.3E-14	1.1E-23
O2	1.2E-06	3.7E-12	5.0E-06	3.3E-09	3.8E-06	5.5E-06	6.3E-10
HS	3.6E-11	4.2E-14	7.1E-11	1.2E-13	2.8E-11	5.0E-13	6.2E-13
*SIC	2.8E-11	2.5E-11	9.5E-12	3.3E-11	5.2E-12	4.1E-11	4.5E-11
*SIO	5.2E-10	1.5E-10	2.7E-10	3.0E-10	2.3E-11	4.3E-10	4.4E-10
CS	6.4E-09	2.6E-16	3.0E-09	7.8E-14	4.8E-10	1.3E-10	1.7E-20
*NS	2.1E-10	3.1E-11	9.1E-11	9.0E-11	2.5E-12	1.2E-10	1.2E-10
SO	1.6E-09	1.4E-15	1.0E-09	6.1E-14	1.1E-10	6.0E-11	3.8E-11
*SIS	1.2E-11	2.1E-12	6.3E-12	5.4E-12	7.2E-14	6.9E-12	6.9E-12
CH2	3.0E-07	1.1E-14	4.7E-08	4.1E-14	5.1E-09	1.3E-14	5.5E-23
NH2	7.6E-09	1.8E-16	2.6E-09	8.1E-17	3.8E-09	3.6E-16	1.6E-24
H2O	1.0E-06	4.5E-05	3.5E-07	1.0E-04	1.7E-07	1.6E-04	1.9E-04
SIH2		1.5E-15		4.6E-15		2.4E-15	2.3E-21
MGH2		6.5E-10		2.7E-09		6.8E-09	1.3E-08
C2H	6.2E-08	7.5E-15	8.4E-09	5.7E-15	3.0E-09	5.9E-15	9.4E-34
N2H		5.1E-11		1.5E-10		3.5E-10	5.2E-10
O2H		6.7E-14		2.7E-15		4.3E-12	4.9E-16
HCN	8.3E-08	1.7E-06	5.5E-09	2.5E-06	1.1E-09	2.5E-06	2.5E-06

t(yr)	1.0E+05		3.2E+05		1.0E+06		1.0E+07
Species	Gas	Surface	Gas	Surface	Gas	Surface	Surface
HNC	4.1E-08	1.9E-07	3.2E-09	2.1E-07	1.0E-09	2.1E-07	2.1E-07
HCO	2.2E-09	9.5E-13	6.8E-10	1.5E-11	4.5E-10	1.4E-11	1.1E-12
HOC		5.8E-12		1.5E-11		1.4E-11	6.2E-23
HCS		6.8E-15		1.0E-14		2.9E-10	5.6E-10
HNO	2.4E-11	3.4E-06	2.4E-12	5.7E-06	1.5E-13	5.8E-06	5.8E-06
H2S	5.3E-11	6.0E-09	9.4E-11	1.3E-08	7.1E-11	7.0E-08	9.1E-08
C3	2.0E-08	3.6E-16	7.9E-09	1.9E-16	1.6E-08	1.2E-15	1.7E-39
O3		1.1E-07		3.4E-07		6.2E-08	2.1E-18
C2N	2.5E-08	2.0E-13	5.7E-09	9.5E-15	7.3E-11	2.2E-14	1.6E-37
*NAOH	4.1E-14	6.3E-15	4.7E-15	1.2E-14	6.5E-16	1.5E-14	1.5E-14
OCN	1.7E-09	6.1E-12	1.3E-09	1.6E-12	1.5E-10	6.8E-10	7.3E-10
CO2	2.6E-07	9.0E-06	1.9E-07	2.3E-05	4.5E-09	2.3E-05	2.3E-05
OCS	4.3E-08	8.4E-09	1.7E-08	2.1E-08	5.4E-10	2.8E-08	2.8E-08
SO2	4.0E-10	1.4E-08	7.8E-11	3.9E-08	2.2E-12	3.9E-08	3.9E-08
CH3	4.9E-09	1.7E-15	5.5E-09	4.4E-14	2.9E-08	7.0E-14	1.3E-22
NH3	1.4E-08	7.9E-09	3.5E-09	1.3E-08	4.5E-09	2.1E-08	3.6E-08
SIH3		1.5E-15		4.6E-15		2.4E-15	2.3E-21
C2H2	2.6E-07	6.2E-08	1.5E-07	8.3E-08	3.7E-08	9.2E-08	2.9E-11
N2H2		1.6E-06		4.7E-06		1.1E-05	1.6E-05
H2O2		1.4E-07		1.6E-07		3.0E-06	7.1E-07
H2CO	1.7E-07	3.9E-06	3.9E-08	7.4E-06	7.7E-09	3.3E-05	4.4E-05
CHOH		5.8E-12		1.5E-11		1.4E-11	6.2E-23
HCCN		2.0E-13		9.5E-15		2.2E-14	1.6E-37
C3H	3.9E-08	1.4E-15	5.6E-09	1.4E-16	1.3E-09	1.6E-16	1.8E-39
*H2CS	1.0E-09	1.0E-10	3.8E-10	3.6E-10	9.8E-12	4.5E-10	4.6E-10
C4	1.7E-08	1.2E-15	5.4E-09	2.5E-15	1.1E-08	1.2E-14	0.0E+00
C3N	2.2E-08	1.2E-13	5.4E-09	6.5E-15	2.8E-10	1.9E-14	1.3E-36
C3O	3.1E-11	4.5E-08	5.3E-11	4.7E-08	3.7E-12	4.7E-08	4.7E-08
CH4	1.8E-06	6.4E-07	1.3E-06	1.9E-06	1.4E-07	2.7E-06	3.8E-06
SIH4		2.9E-09		7.7E-09		1.4E-08	1.6E-08
C2H3	5.4E-08	3.4E-14	1.4E-08	7.0E-14	4.1E-09	7.4E-14	2.1E-17
*CH3N	8.7E-10	1.5E-10	2.6E-11	2.9E-10	5.7E-12	3.0E-10	3.1E-10
C3H2	2.4E-08	7.9E-09	7.3E-09	5.9E-09	1.7E-09	4.3E-09	1.5E-12
C2H2N	2.8E-08	2.0E-13	9.7E-10	1.0E-14	1.2E-11	2.2E-14	1.6E-37
*C2H2O	3.6E-08	5.7E-09	2.9E-09	1.1E-08	5.4E-11	1.2E-08	1.2E-08
*CH2O2	1.0E-09	8.5E-11	1.1E-09	5.2E-10	7.4E-11	1.0E-09	1.1E-09
CH2OH		5.8E-12		1.5E-11		1.4E-11	6.2E-23
C4H	1.2E-07	1.3E-14	1.0E-08	7.3E-15	1.9E-09	1.4E-14	0.0E+00
HC3N	5.8E-08	1.7E-07	5.5E-09	9.3E-08	1.8E-10	4.4E-08	1.3E-11
C5	8.7E-09	2.2E-16	1.5E-09	2.8E-17	1.9E-09	1.1E-16	0.0E+00
*C4N	2.9E-09	3.1E-10	4.1E-10	7.6E-10	8.0E-12	8.4E-10	8.5E-10
C2H4	1.2E-09	2.3E-09	7.6E-10	4.5E-09	2.2E-11	5.0E-09	1.5E-12
CH3OH	3.2E-09	1.3E-05	1.2E-10	3.0E-05	1.0E-11	5.5E-05	6.6E-05
C3H3	1.8E-10	2.5E-14	6.8E-11	4.4E-15	2.0E-12	3.2E-15	1.1E-18
C2H3N	3.7E-09	7.0E-07	2.1E-11	9.1E-07	7.8E-13	9.2E-07	9.6E-07
C3H2N		1.2E-13		6.8E-14		3.2E-14	9.3E-18

TABLE 8—*Continued*

t(yr)	1.0E+05		3.2E+05		1.0E+06		1.0E+07
Species	Gas	Surface	Gas	Surface	Gas	Surface	Surface
C4H2	2.0E-08	1.7E-08	3.5E-09	1.6E-08	1.9E-10	1.3E-08	6.7E-12
C5H	4.2E-09	9.8E-17	1.8E-10	4.5E-18	1.2E-11	7.2E-18	0.0E+00
C6	3.4E-09	2.4E-16	3.6E-10	1.4E-16	2.3E-10	2.0E-16	0.0E+00
C5N	2.9E-09	1.3E-15	3.8E-10	7.6E-16	6.5E-12	1.7E-15	0.0E+00
*CH5N	6.4E-10	1.0E-10	1.9E-11	2.0E-10	3.8E-12	2.1E-10	2.2E-10
C2H5		3.4E-14		6.7E-14		7.4E-14	2.3E-17
C3H4	2.3E-10	1.9E-07	2.5E-10	2.2E-07	4.8E-12	2.2E-07	2.3E-07
C4H3		1.2E-14		1.2E-14		9.9E-15	5.0E-18
*C2H4O	1.4E-11	1.7E-12	2.5E-12	4.3E-12	1.9E-13	5.1E-12	5.3E-12
C3H3N	2.0E-10	2.9E-07	2.0E-11	4.7E-07	4.5E-14	5.4E-07	6.3E-07
C5H2	4.4E-09	5.6E-10	4.2E-10	5.1E-10	1.2E-11	2.1E-10	3.0E-14
C6H	2.0E-09	4.0E-16	6.9E-11	1.7E-16	3.5E-12	2.0E-16	0.0E+00
HC5N	5.1E-09	2.1E-09	1.9E-10	2.2E-09	9.4E-13	1.7E-09	5.7E-13
C7	1.5E-09	3.8E-17	1.3E-10	2.0E-18	5.7E-11	2.8E-18	0.0E+00
*CH3C3N	3.7E-10	4.7E-11	8.4E-12	7.8E-11	3.2E-14	7.9E-11	7.9E-11
C5H2N		1.5E-15		1.6E-15		1.2E-15	4.2E-19
C2H6		3.2E-07		3.9E-07		5.1E-07	7.2E-07
C4H4		4.8E-08		7.0E-08		8.5E-08	1.3E-07
C5H3		4.1E-16		3.8E-16		1.6E-16	2.2E-20
C6H2	4.5E-09	7.8E-10	6.9E-10	7.9E-10	4.0E-11	4.6E-10	1.0E-13
C7H	1.1E-09	2.0E-17	1.9E-11	3.8E-19	7.5E-13	2.0E-19	0.0E+00
C8	7.9E-10	4.7E-17	4.2E-11	1.4E-17	1.9E-11	1.5E-17	0.0E+00
C7N	5.4E-10	2.2E-16	2.6E-11	5.1E-17	2.7E-13	4.4E-17	0.0E+00
*CH3OCH3	3.0E-12	2.6E-13	1.8E-14	6.2E-13	1.5E-16	6.2E-13	6.2E-13
*C2H5OH	2.9E-12	2.2E-13	7.4E-13	9.5E-13	8.4E-15	1.1E-12	1.1E-12
*CH3C4H	3.3E-09	2.4E-10	3.8E-10	8.4E-10	6.1E-12	8.9E-10	9.0E-10
C5H4		3.6E-09		4.3E-09		4.7E-09	5.0E-09
C6H3		5.7E-16		5.8E-16		3.4E-16	7.5E-20
C7H2	9.3E-10	1.1E-10	2.8E-11	6.8E-11	9.5E-13	2.5E-11	2.7E-15
C8H	1.1E-09	1.2E-16	1.5E-11	1.9E-17	6.4E-13	1.5E-17	0.0E+00
HC7N	1.1E-09	3.9E-10	2.3E-11	3.1E-10	1.7E-13	1.4E-10	2.4E-14
C9	2.2E-10	6.9E-18	1.0E-11	1.4E-19	3.1E-12	1.3E-19	0.0E+00
C5H3N		3.8E-09		6.8E-09		8.7E-09	1.3E-08
*CH3C5N	2.6E-11	2.6E-12	1.2E-13	4.0E-12	1.1E-16	4.0E-12	4.0E-12
C7H2N		2.9E-16		2.3E-16		1.0E-16	1.8E-20
C6H4		2.3E-09		3.3E-09		4.0E-09	4.9E-09
C7H3		8.0E-17		5.0E-17		1.9E-17	2.0E-21
C8H2	5.5E-10	1.8E-10	4.1E-11	1.3E-10	3.1E-13	5.6E-11	1.1E-14
C9H	1.4E-10	2.7E-18	9.8E-13	2.0E-20	1.0E-14	8.3E-21	0.0E+00
C9N	6.9E-11	3.7E-17	1.5E-12	3.4E-18	2.7E-15	2.1E-18	0.0E+00
*CH3C6H	9.5E-11	6.2E-12	3.5E-12	1.6E-11	1.8E-14	1.7E-11	1.7E-11
C7H4		5.2E-10		6.5E-10		7.0E-10	7.2E-10
C8H3		1.4E-16		9.6E-17		4.1E-17	8.2E-21
C9H2	2.1E-10	1.9E-11	2.0E-12	1.1E-11	1.3E-14	3.9E-12	3.6E-16
HC9N	1.3E-10	6.6E-11	1.3E-12	4.1E-11	1.7E-15	1.6E-11	1.9E-15
C7H3N		5.9E-10		1.1E-09		1.3E-09	1.5E-09
*CH3C7N	5.3E-12	4.8E-13	1.3E-14	7.3E-13	1.8E-17	7.3E-13	7.3E-13
C9H2N		4.9E-17		3.0E-17		1.2E-17	1.4E-21
C8H4		3.7E-10		5.9E-10		6.8E-10	7.8E-10
C9H3		1.4E-17		8.1E-18		2.8E-18	2.6E-22
C9H4		5.4E-11		7.5E-11		8.3E-11	8.7E-11
C9H3N		9.7E-11		1.7E-10		2.0E-10	2.2E-10
E	3.6E-08		4.1E-08		5.2E-08		
H+	3.0E-10		8.4E-10		1.5E-09		
HE+	6.4E-10		8.3E-10		2.7E-09		
C+	2.9E-09		8.0E-09		8.4E-09		
N+	5.6E-12		2.6E-12		4.2E-12		
O+	2.3E-15		1.4E-14		2.4E-14		
NA+	2.9E-09		2.4E-09		1.7E-09		
MG+	9.5E-09		8.0E-09		5.4E-09		
SI+	1.4E-11		3.6E-11		9.3E-12		
S+	2.0E-10		6.5E-10		1.1E-10		
FE+	4.8E-09		4.7E-09		4.5E-09		
O2+	9.1E-12		1.0E-10		1.2E-10		
CH+	1.8E-13		1.6E-14		3.0E-15		
SO+	1.3E-11		2.4E-11		6.9E-12		
H3+	2.2E-09		4.0E-09		1.9E-08		
HCO+	5.2E-09		8.1E-09		6.4E-09		
HOC+	4.9E-10		5.8E-10		4.5E-10		
N2H+	5.6E-13		4.9E-12		2.1E-11		
HCS+	2.0E-11		3.8E-11		2.3E-11		
OCS+	2.0E-10		1.4E-10		5.0E-12		
H3O+	2.0E-09		1.3E-09		1.1E-09		
HCO2+	4.5E-12		6.6E-12		7.3E-13		
H2CN+	4.1E-10		5.6E-11		3.3E-11		
NH4+	4.7E-11		1.6E-11		3.5E-11		
CH5+	4.0E-10		2.0E-10		1.1E-10		
C4H2+	4.0E-10		8.1E-11		3.2E-11		
GRAIN0	1.3E-14		1.6E-14		2.5E-14		
GRAIN-	2.6E-12		2.6E-12		2.6E-12		

NOTES.—An asterisk indicates that a species is formed by accretion only. Numbers less than 1×10^{-39} have been truncated and are presented as 0.0. For some molecules, results are given for all isomers and for one particular isomer, e.g., C_5H_4 and CH_3C_4H.

under the influence of gravitation as the preaccretion gaseous chemistry evolved. That hydrogenation on grains is not the only chemistry occurring seems to be revealed by the recent observation of the unsaturated gaseous molecule C_2H_2 (Evans, Lacy, & Carr 1991).

4.1. *Comparison with Other Models*

Comparison with other models is rendered difficult by differing assumptions regarding chemical networks and rates, time dependence, and initial conditions. In Table 9 are listed selected results from three previous calculations—those of TH, d'Hendecourt et al. (1985), and Brown (1990)—and analogous results from our models. We compare only surface compositions, expressed as molecule or mole percentage. All of the results shown in Table 9 are derived for dark clouds with parameters similar to our own.

The results of TH are not strictly time-dependent, since they utilize steady state gaseous abundances. In our model A we commence with such abundances, and the gas phase shows relatively steady state behavior until depletion sets in. We therefore utilize our surface results at 1×10^5 yr to compare with those of TH (specifically their ζ Oph model). Both models show water and CO_2 to be very abundant species; our model contains more CO and O_2 due to higher H levels in TH. The N_2 abundances are very similar, although our inclusion of N_2 hydrogenation via H atoms leads to an appreciable N_2H_2 abundance as well. Methanol, an appreciable surface component in our model, was not listed by TH. Given differences in hydrogenation between models, it is useful to compare sums of abundances of important diatomic molecules and their assorted hydrogenated forms. For CO, the relevant sum, referred to as COH_x in Table 9, consists of the abundances of CO, HCO, H_2CO, and CH_3OH. For N_2 and O_2, the sums, referred to as N_2H_x and O_2H_x, respectively, consist of the bare diatomic species and the singly and doubly hydrogenated forms (e.g., HO_2 and H_2O_2). As can be seen in Table 9, the summed abundances are in good agreement for the ζ Oph model of TH and our early-time model A.

The time-dependent results of d'Hendecourt et al. (1985) can be compared with those of our model B, which has similar, H-rich, initial conditions. Although d'Hendecourt et al. (1985) utilized nonthermal desorption in their so-called standard model, they also presented results for a model in which such desorption was not considered. It is these latter results that are shown in Table 9. Comparison is made at the asymptotic time of 1×10^7 yr. Calculated abundances of the dominant species methane, ammonia, and water are in good agreement. Severe discrepancies are found, however, for CO, N_2, and O_2, for which our calculated asymptotic values are many orders of magnitude lower. These differences are partially due to our more efficient hydrogenation reactions for these species,

TABLE 9

SELECTED COMPARISONS WITH PREVIOUS GAS-GRAIN AND GRAIN CHEMICAL MODELS: SURFACE COMPOSITION (% by number)

Species	TH[a] (ζ Oph)	Model A (1×10^5 yr)	d'H[b] (1×10^7 yr)	Model B (1×10^7 yr)	Brown[c] Case 3	Model C (1×10^7 yr)
H_2	...	7		1	...	1
CO	0.25	10	10	5(−13)	29	2(−11)
N_2	5.4	5	0.1	4(−17)	4.9	1(−04)
O_2	0.74	10	0.3	1(−15)	6.4	2(−04)
H_2O	58	20	65	60	44	40
CO_2	5.2	20	0.4	7	1.4(−3)	40
NH_3	0.70	0.04	9.3	8	6.8	0.01
H_2CO	25	10	...	7	9.9(−04)	5
H_2O_2	2.0	6	...	1(−05)	8.8	0.3
N_2H_2	...	3	...	0.9	...	6
CH_4	4(−03)	7(−02)	14	10	0.14	1
CH_3OH	...	10	...	7	1.1	5
COH_x[d]	25	30	10	10	30	10
N_2H_x[d]	5.4	7.0	0.1	0.9	4.9	6
O_2H_x[d]	8.9	20	0.3	1(−05)	15	0.3
C_2H_2	...	...	...	...	0.27	1(−5)
C_2H_4	...	...	...	...	0.017	5(−07)
C_2H_6	...	...	...	...	2.6(−03)	0.3
HCN	...	...	...	...	0.29	1
CH_3NH_2	...	...	...	...	0.18	*8(−05)*
CH_3CHO	...	...	...	...	0.031	*2(−06)*
C_2H_5OH	...	...	...	...	0.11	*4(−07)*
CH_3OCH_3	...	...	...	...	0.011	*2(−07)*

NOTES.—$a(-b)$ means $a \times 10^{-b}$. Italics refer to species formed only by accretion from the gas. Our results rounded off to one significant figure.

[a] Tielens & Hagen 1982.

[b] d'Hendecourt et al. 1985; test model without nonthermal desorption.

[c] Brown 1990.

[d] Refers to the sum of basic species (e.g., CO) plus all hydrogenated forms (e.g., H_2CO).

as can be seen by comparing the summed abundances COH_x and N_2H_x. Our low value for O_2H_x is due to the destruction of H_2O_2 by H atoms.

The grain chemical model of Brown (1990), like our own, is concerned primarily with the production of organic molecules, and his case 3 can be compared with our asymptotic model C results, in which H_2-rich initial conditions are utilized. However, in addition to differences in the hydrogenation rate of basic molecules, Brown (1990) employs a very different surface reaction scheme for complex molecule development, based on AR and discussed earlier, in which radicals react with one another efficiently with the same rate coefficient. In addition, Brown (1990) is most interested in oxygen-containing organics, such as found in the Orion compact ridge (Millar et al. 1991), whereas our concern is mainly with the synthesis of hydrocarbons and organo-nitrogen species. A final difference is that Brown (1990) allows ejection into the gas following formation on grain surfaces for selected species. The limited comparison that can be made shows that for hydrocarbons our species tend to be more saturated (since we allow H atom addition reactions with activation energy), and that for oxygen-containing organics Brown (1990) obtains much greater abundances, since our oxygen-containing molecules on grain surfaces are formed only via accretion from the gas. The different abundances obtained by us and Brown (1990) for complex molecule abundances point out most vividly the consequences of the continuing uncertainty in surface reaction rates.

4.2. *Comparison with Observations in TMC-1*

There are no observations available of solid phase molecules exactly in the direction of TMC-1, which is a very small part of the Taurus dark cloud complex. There are, however, various measurements of spectral features at 3.1, 4.7, and 9.7 μm attributed to ice, CO, and silicate solid/surface phase molecules directed toward about a dozen embedded and background IR sources in the region of the Taurus dark cloud (Whittet & Duley 1991). The ratio of column densities between surface and gaseous CO based on the 4.7 μm feature is of order $\frac{1}{4}$ and is fairly constant over the Taurus region. We therefore assume that this abundance ratio applies to TMC-1, leading to an abundance ratio between surface CO and gaseous H_2, $n_s(CO)/n(H_2)$, of approximately a few times 10^{-5}. An abundance ratio between surface CO and surface water ice of ≈ 0.2 in the Taurus region can also be inferred based on observations of Whittet et al. (1988, 1989) and laboratory data of Sandford et al. (1988). A successful model must reproduce these ratios as well as the large number of gas-phase abundances. The gas-phase abundances are best reproduced at early times [$(1\text{–}3) \times 10^5$ yr] by a model in which the starting abundances are either the standard ones, i.e., those of models C and D, or neutral atoms, i.e., model B. Model B does contain peak abundances of gaseous organic molecules that can be too low, especially for the most complex ones in the model, although it is not clear that overall it is any worse than models C and D at early times (Pineau des Forêts et al. 1991). Model A, which commences with steady state gaseous abundances, contains very low abundances of complex gaseous molecules, despite a small rise at 1×10^6 yr. Comparison of surface observations in Taurus with results from models A, B, C, and D are contained in Table 10 in the form of abundance ratios [CO(ice)/CO(gas), CO(ice)/H_2(gas), CO(ice)/H_2O(ice)]. Of the models (B, C, and D) that are in reasonable agreement with the observed gas-phase abundances at early times, models B and C can be eliminated because of the very low predicted surface abundance of CO, due essentially to rapid conversion into CO_2. Model D, in which the CO $\rightarrow$ CO_2 conversion does not occur, is in good agreement with the observations of surface CO and ice. A modified model B, in which the CO + O reaction is turned off, might reproduce the surface observations as well but would lead to the prediction of much larger surface abundances of saturated molecules such as CH_4 and NH_3.

4.3. *Comparison with Surface Observations in Other Regions*

In addition to the data from Taurus, Table 10 contains data from three other IR sources in molecular clouds (Whittet & Duley 1991), in which CH_4 has also been detected both in the gas and probably on dust surfaces (Lacy et al. 1991). Two additional abundance ratios—CH_4(tot)/CO(tot) and CH_4(ice)/CO(ice)—can be investigated. Two of the sources contain lower abundances of surface CO than found in Taurus, perhaps due to higher temperatures and radiative desorption. Nevertheless, the observations of all three sources are compared with results from our dark cloud gas-grain models A, B, C, and D in Table 10. Of these models, once again model D appears to reproduce the data best, coming within an order of magnitude of the assorted ratios at early times, although, if one ignores gas-phase abundances, model A cannot be ruled out. Models B and C contain far too little surface CO, except perhaps at 1×10^6 yr. Modification of model B by removal of the CO + O $\rightarrow$ CO_2 reaction would still probably leave the problem of too great a predicted surface methane abundance.

Tielens (1989) has given a representative picture of icy grain mantles in ambient interstellar sources. Although not referring to one specific source, the average surface molecular abundances presented by Tielens are useful for comparison. Table 11 contains some of these abundances normalized to water ice (set at 100) along with our computed values from model D at both 1×10^5 and 3×10^5 yr. The agreement is very good for the molecules CH_3OH (which possesses a very large abundance) and H_2S; in addition, our computed abundances for methane and ammonia do not disagree strongly with the upper limits presented. The only problem is for formaldehyde, where our computed abundances are much too high, implying that hydrogenation to methanol is more efficient than in our model.

Whittet & Walker (1991) have noted that when the 4.7 μm CO feature appears with a relatively narrow line width, it derives from dust particles that are not dominated by polar species such as water ice. Tielens et al. (1991) have shown that along many lines of sight both a narrow CO feature from a nonpolar solid environment and a broader CO feature from a polar, probably water-ice–dominated environment are present. In W33A, for example, they find that roughly one-third of the surface CO resides on grains that are nonpolar. Since our models yield grain surfaces in which water ice is a major if not always dominant component, it would appear that our results cannot account for the narrow CO feature.

TABLE 10

COMPARISON WITH SURFACE OBSERVATIONS TOWARD LUMINOUS IR SOURCES

Object/Model	CO(ice)/CO(gas)	CO(ice)/H_2(gas)	CO(ice)/H_2O(ice)	CH_4(tot)/CO(tot)	CH_4(ice)/CO(ice)
Observations					
Taurus[a]	0.25[c]	2.9(−5)[b,c]	0.2[c]	...	...
7538 IRS 9[d]	0.10	...	0.24[e]	0.013	0.13
7538 IRS 1[d]	0.0057	...	0.028[e]	0.010	3.3
W33A[d,f]	0.035	2.8(−6)[f]	0.007[f]	0.044	2.4
Models					
Model A:					
1×10^5 yr	0.061	7.3(−6)	0.66	0.0012	0.0059
3×10^5	0.21	1.5(−5)	0.52	0.0023	0.0073
1×10^6	0.73	1.1(−5)	0.19	0.018	0.031
Model B:					
1×10^5	5.6(−8)	2.4(−12)	2.9(−8)	0.79	1.4(+7)
3×10^5	2.4(−6)	1.3(−10)	9.3(−7)	0.98	4.0(+5)
1×10^6	0.083	9.9(−7)	0.0045	4.2	55
Model C:					
1×10^5	4.0(−8)	2.7(−12)	9.3(−8)	0.039	3.0(+5)
3×10^5	0.014	8.3(−8)	0.013	0.057	25
1×10^6	0.42	5.4(−6)	0.063	0.17	0.54
Model D:					
1×10^5	0.066	4.4(−6)	0.098	0.034	0.15
3×10^5	0.20	1.2(−5)	0.12	0.044	0.16
1×10^6	0.77	1.0(−5)	0.063	0.12	0.27

[a] Whittet & Duley 1991.

[b] $N(H_2)$ (cm^{-2}) = 1×10^{21} A_V(mag) is assumed.

[c] A(pure H_2O, 3 μm) = 2×10^{-16} cm $mole^{-1}$, A(CO–H_2O mixture, 4.67 μm) = 1.7×10^{-17} cm $mole^{-1}$ (Sandford et al. 1988); FWHM (3 μm) = 325 cm^{-1}, and FWHM (4.67 μm) = 7.7 cm^{-1} (Whittet et al. 1988, 1989) are assumed.

[d] Lacy et al. 1991 and Mitchell et al. 1990

[e] Willner et al. 1982 with A(pure H_2O, 3 μm).

[f] Tielens et al. 1991; both CO components counted.

TABLE 11

COMPARISON WITH "TYPICAL" SURFACE ABUNDANCES

Species	Observed[a]	Model D, 1×10^5 yr	Model D, 3×10^5 yr
H_2O	100	100	100
CH_3OH	7, 50[b]	29	30
NH_3	<5	0.02	0.01
H_2S	0.3	0.01	0.01
CH_4[c]	<1	1.4	1.9
H_2CO	<0.2	8.7	7.4
H_2O(ice)/H_2(gas)	...	4.5(−05)	1.0(−04)

NOTES.—$a(-b)$ means $a \times 10^{-b}$. Surface abundances normalized relative to H_2O = 100.

[a] Tielens 1989.

[b] Two different estimates given.

[c] Observed values of 3–9 are consistent with the more recent results in Table 10.

4.4. *Comparison with the Orion Hot Core*

Some of the most concrete signatures of grain chemistry to date have been found in star-forming regions, such as the hot core and compact ridge of Orion. The hot core in particular, with its large abundances of hydrogenated species and their deuterated isotopomers, seems to betray the signature of an atomic-hydrogen–rich grain chemistry followed by evaporation into the gas. A model along such lines has been constructed by Brown et al. (1988). Although our model has been created to represent more quiescent regions, we can make the additional assumption of a sudden desorption of surface molecules into the gas to compare our results with observations of the Orion hot core (or the compact ridge; see Millar et al. 1991). This is a crude physical assumption and involves the further approximation that the chemistry does not change rapidly after the sudden desorption, a point considered in detail by Brown et al. (1988). In Table 12 some observations of molecular abundances in the hot core are compared with results from two of our models, B and D, at optimum (early) times. For completeness, early-time purely gas-phase results as well as the results of Brown et al. (1988) are included. The large abun-

TABLE 12

COMPARISON WITH OBSERVATIONS OF THE ORION HOT CORE

Species	Observed[a]	BCM[b]	Model B (3×10^5 yr)	Model D (1×10^5 yr)	Gas Model[c] (1×10^5 yr)
C	<4.5(−7)	9.2(−11)	4.4(−6)	3.7(−5)	5.4(−5)
CO	1.2(−4)	1.7(−4)	5.4(−5)	7.1(−5)	8.5(−5)
CS	<5.5(−10)	...	2.0(−9)	6.4(−9)	8.9(−9)
SO	<2.0(−8)	...	7.1(−10)	1.6(−9)	1.7(−9)
O_2	<1(−4)	...	3.2(−6)	1.2(−6)	9.3(−7)
H_2O	>5.3(−6)	9.2(−4)	1.7(−4)	4.6(−5)	1.3(−6)
H_2S	5(−6)[d]	...	6.6(−8)	6.1(−9)	5.0(−11)
C_2H	<5.5(−10)	8.2(−7)	9.9(−9)	6.2(−8)	7.0(−8)
CO_2	<1(−5)	...	2.8(−6)	9.3(−6)	3.5(−7)
SO_2	<2.4(−8)	...	2.4(−10)	1.4(−8)	5.7(−10)
HCN	3.0(−7) 0.5–5(−6)[e]	1.1(−7)	4.4(−8)	1.8(−6)	1.3(−7)
HNO	...	...	5.5(−9)	3.4(−6)	3.3(−11)
OCS	0.9–5(−6)[e]	...	1.5(−8)	5.1(−8)	6.3(−8)
NH_3	1.0(−5)	2.2(−4)	2.7(−5)	2.2(−8)	1.6(−8)
H_2CO	2.6(−8)	2.2(−7)	1.5(−5)	4.1(−6)	1.9(−7)
C_2H_2	0.3–6(−6)[e]	...	1.4(−7)	3.2(−7)	3.0(−7)
H_2O_2	<5(−10)	...	1.1(−10)	1.4(−7)	...
CH_4	<1(−5) 1(−7)–3(−6)[f]	2.0(−4)	5.3(−5)	2.4(−6)	2.1(−6)
HC_3N	1.6(−9)	1.7(−9)	5.1(−9)	2.3(−7)	7.9(−8)
CH_3CN	7.8(−9)	2.4(−8)	3.0(−9)	7.0(−7)	6.3(−9)
CH_3OH	...	...	1.5(−5)	1.3(−5)	4.2(−9)
C_2H_3CN	1.8(−9)	...	5.7(−9)	2.9(−7)	1.9(−11)
HCO^+	<4.5(−10)	4.4(−14)	6.7(−9)	5.2(−9)	5.0(−9)

NOTES.—$a(-b)$ means $a \times 10^{-b}$. Fractional abundances are relative to $H_2 + 0.5H$.

[a] Blake et al. 1987 unless indicated.

[b] Brown et al. 1988. Model B (carbon initially in the form of C^+).

[c] Herbst & Leung 1989. No accretion. Initial conditions are the same as in models C and D.

[d] Minh et al. 1990.

[e] Evans et al. 1991.

[f] This is our estimate based on data of Lacy et al. 1991.

dances of hydrogenated species (e.g., H_2S, NH_3) in the hot core are of course best represented by our H-rich model (model B) and that of Brown et al. (1988). In addition, model B reproduces adequately the abundances of the partially hydrogenated species C_2H_2, CH_3CN, and C_2H_3CN. However, quantitative agreement between model B and observation is still lacking for a variety of species. For example, the H_2S abundance, despite a significant enhancement vis-à-vis the other models, is underestimated considerably, and that of H_2CO is even more seriously overestimated. Also, our calculated abundance of HCO^+ is much too high in all models, since our gas density is too low to represent the ionic balance adequately.

5. SUMMARY

To represent the chemistry of cool interstellar clouds, we have presented a variety of model results based on a large chemical network of gas-phase reactions augmented with a grain-surface chemistry based on the ideas of earlier authors, mainly Tielens and collaborators (TH; TA), in which atom-radical reactions dominate. Quantitative estimates for the rates of processes occurring on grain surfaces have been attempted, albeit with large uncertainties. The models we present can be considered as extensions of our previous pseudo–time-dependent gas-phase calculations, in that the temperature is fixed and the gas density is roughly constant. Particular attention is paid to the synthesis of large organic molecules on grain surfaces. In the models, only thermal desorption is considered, so that for cool sources, neutral heavy species will all eventually reside on the grain surfaces. However, for times considerably shorter than this, a significant gas phase is still present, and both gas-phase and surface chemistry occur. In particular, the products of gas-phase syntheses can be important ingredients in subsequent syntheses on the surfaces of dust particles.

Four different models have been considered, differing mainly in their initial gas-phase composition. Differences between our calculated results and those of previous gas-grain and grain models demonstrate the continuing large uncertainties present in grain chemistry. The model results have also been compared with observations of both surface and gas-phase molecules. The limited nature of current observations of surface molecules precludes detailed comparison with most of our predictions concerning surface syntheses of large molecules. From IR observations of surface CO, CH_4, and water ice in selected regions and their relative strengths with respect to gas-phase features, we determine that an early-time gas-grain model (model D) incorporating the standard initial conditions used in our previous purely gas-phase models (H in the form of H_2, atoms such as C, S, and Si singly ionized) seems to represent adequately both the gaseous chemistry in the molecule factory TMC-1 as well as surface observations over wider regions in Taurus and other regions, as long as the surface reac-

tion $CO + O \rightarrow CO_2$ is excluded. An alternative model (model B), in which totally neutral atomic abundances are utilized as initial conditions, cannot be ruled out, although it leads to smaller abundances of complex gas-phase molecules. One newly found feature (Tielens et al. 1991) that our surface models cannot reproduce is the apparent bifurcation along many lines of sight of surface CO into molecules found on ice-dominated surfaces such as those calculated here and molecules found on nonpolar surface environments. Reproduction of this duality of surface features along given lines of sight would require (*a*) less efficiency in the production of surface H_2O in our H-poor models and (*b*) a reason why the different regions differ in their initial gaseous compositions.

Because detailed evidence for surface chemistry is found in star-forming regions such as the Orion hot core, we have also compared our results with observations directed toward this region. Because the comparison is a crude one for several reasons, our results cannot be expected to be more than semiquantitative and suggestive. We find that the unique aspects of the hot core chemistry are best explained by the H I–rich model (model B) at early times, in which copious amounts of gaseous atomic hydrogen are present to accrete and form saturated surface molecules. Desorption then places these saturated molecules in a gas phase already full of unsaturated species present in significant abundance at early times. Interestingly, this model (without instantaneous desorption) is not best for the dark cloud TMC-1, at least for the complex molecules found in it, because the gas-phase synthetic processes are less efficient than if H_2 is the initial form of hydrogen. The requirement for different initial conditions in different types of sources is puzzling but may be indicative of the physical processes occurring in cloud formation. More refined calculations on star-forming regions are planned.

E. H. acknowledges the support of the National Science Foundation for his research program in astrochemistry. He also wishes to thank the North Carolina Supercomputing Center for computer time on their Cray Y-MP4, and the Ohio Supercomputer Center for computer time on their Cray Y-MP8, where much of the necessary computing was performed.

REFERENCES

Aannestad, P. 1973, ApJS, 25, 505
Allen, M., & Robinson, G. W. 1975, ApJ, 195, 81
———. 1976, ApJ, 207, 745
———. 1977, ApJ, 212, 396 (AR)
Blake, G. A., Sutton, E. C., Masson, C. R., & Phillips, T. G. 1987, ApJ, 315, 621
Breukers, R. J. L. H. 1991, Ph.D. thesis, University of Leiden
Brown, P. D. 1990, MNRAS, 243, 65
Brown, P. D. & Charnley, S. B. 1990, MNRAS, 244, 432
———. 1991, MNRAS, 249, 69
Brown, P. D., Charnley, S. B., & Millar, T. J. 1988, MNRAS, 231, 409
Brown, P. D., & Millar, T. J. 1989a, MNRAS, 237, 661
———. 1989b, MNRAS, 240, 25P
Charnley, S. B., Dyson, J. E., Hartquist, T. W., & Williams, D. A. 1988, MNRAS, 231, 269
Chièze, J.-P., Pineau des Forêts, G., & Herbst, E. 1991, ApJ, 373, 110
Cowfer, J. A., Keil, D. G., Michael, J. V., & Yeh, C. 1971, J. Phys. Chem., 75, 1584
Daby, E. E., Niki, H., & Weinstock, B. 1971, J. Phys. Chem., 75, 1601
d'Hendecourt, L. B., Allamandola, L. J., & Greenberg, J. M. 1985, A&A, 152, 130
Evans, N. J., II, Lacy, J. H., & Carr, J. S. 1991, ApJ, 383, 674
Federman, S. R., & Allen, M. 1991, ApJ, 375, 157
Grim, R. J. A., & d'Hendecourt, L. B. 1986, A&A, 167, 161
Herbst, E. 1990, Angew. Chem. Int. Ed., 29, 595
Herbst, E., & Leung, C. M. 1986, ApJ, 310, 378
———. 1989, ApJS, 69, 271 (HL1)
———. 1990, A&A, 233, 177 (HL2)
Herbst, E., & Millar, T. J. 1991, in Molecular Clouds, ed. R. James & T. J. Millar (Cambridge: Cambridge Univ. Press), 209
Hollenbach, D., & Salpeter, E. E. 1970, J. Chem. Phys., 53, 79
Knacke, R. F., & Larson, H. P. 1991, ApJ, 367, 162
Lacy, J. H., Baas, F., Allamandola, L. J., Persson, S. E., McGregor, P. J., Lonsdale, C. J., Geballe, T. R., & van de Bult, C. E. P. 1984, ApJ, 276, 533
Lacy, J. H., Carr, J. S., Evans, N. J., II, Baas, F., Achtermann, J. M., & Arens, J. F. 1991, ApJ, 376, 556
Léger, A., Jura, M., & Omont, A. 1985, A&A, 144, 147
Leung, C. M., Herbst, E., & Huebner, W. F. 1984, ApJS, 56, 231
Meyer, D. M., & Roth, K. C. 1991, ApJ, 376, L49
Millar, T. J., Herbst, E., & Charnley, S. B. 1991, ApJ, 369, 147
Millar, T. J., Leung, C. M., & Herbst, E. 1987, A&A, 183, 109
Minh, Y. C., Ziurys, L. M., Irvine, W. M., & McGonagle, D. 1990, ApJ, 360, 136
Mitchell, G. F. 1984, ApJS, 54, 81
Mitchell, G. F., & Deveau, T. J. 1983, ApJ, 266, 646
Mitchell, G. F., Maillard, J.-P., Allen, M., Beer, R., & Belcourt, K. 1990, ApJ, 363, 554
Pauls, T. A., Wilson, T. L., Bieging, J. H., & Martin, R. N. 1983, A&A, 124, 123
Payne, W. A., & Stief, L. J. 1976, J. Chem. Phys., 64, 1150
Penzhorn, R. D., & Darwent, B. de B. 1971, J. Chem. Phys., 55, 1508
Pineau des Forêts, G., Flower, D. R., & Herbst, E. 1991, MNRAS, 253, 359
Prasad, S. S., Heere, K. R., & Tarafdar, S. P. 1991, ApJ, 373, 123
Sandford, S. A., & Allamandola, L. J. 1990, ApJ, 355, 357
Sandford, S. A., Allamandola, L. J., Tielens, A. G. G. M., & Valero, G. J. 1988, ApJ, 329, 498
Schatz, G. C., Koizumi, H., & Lendvay, G. 1991, in Isotope Effects in Chemical Reactions and Photodissociation Processes, ed. J. A. Kaye (Washington, DC: ACS Books), in press
Scheer, M. D., & Klein, R. 1961, J. Phys. Chem., 65, 375
Tielens, A. G. G. M. 1989, in Interstellar Dust, ed. L. J. Allamandola & A. G. G. M. Tielens (Dordrecht: Kluwer), 239
Tielens, A. G. G. M. & Allamandola, L. J. 1987, in Interstellar Processes, ed. D. J. Hollenbach & H. A. Thronson, Jr. (Dordrecht: Kluwer), 397 (TA)
Tielens, A. G. G. M., & Hagen, W. 1982, A&A, 114, 245 (TH)
Tielens, A. G. G. M., Tokunaga, A. T., Geballe, T. R., & Baas, F. 1991, ApJ, 381, 181
Turner, B. E. 1990, ApJ, 362, L29
Walmsley, C. M., Hermsen, W., Henkel, C., Mauersberger, R., & Wilson, T. L. 1987, A&A, 172, 311
Watson, W. D. 1976, Rev. Mod. Phys., 48, 513
Watson, W. D., & Salpeter, E. E. 1972a, ApJ, 174, 321
———. 1972b, ApJ, 175, 659
Whittet, D. C. B., Adamson, A. J., Duley, W. W., Geballe, T. R., & McFadzean, A. D. 1989, MNRAS, 241, 707
Whittet, D. C. B., Bode, M. F., Longmore, A. J., Adamson, A. J., McFadzean, A. D., Aitken, D. K., & Roche, P. F. 1988, MNRAS, 233, 321
Whittet, D. C. B., & Duley, W. W. 1991, A&A Rev., 2, 167
Whittet, D. C. B., & Walker, H. J. 1991, in Molecular Clouds, ed. R. A. James & T. J. Millar (New York: Cambridge Univ. Press), 309
Willner, S. P., et al. 1982, ApJ, 253, 174